Materials Today xxx (xxxx) xxx

Contents lists available at ScienceDirect

Materials Today

journal homepage: www.elsevier.com/locate/mattod

Triboelectric nanogenerators as a clean energy scavenging technology

Ya Yang [a,b,1], Jie Wang [a,b,1], Weiqi Qian [a,b], Zhong Lin Wang [a,c,*]

[a] Beijing Key Laboratory of Micro-Nano Energy and Sensor, Center for High-Entropy Energy and Systems, Beijing Institute of Nanoenergy and Nanosystems, Chinese Academy of Sciences, Beijing, China
[b] School of Nanoscience and Technology, University of Chinese Academy of Sciences, Beijing, China
[c] School of Materials Science and Engineering, Georgia Institute of Technology, Atlanta, GA, United States

ARTICLE INFO

Keywords:
Triboelectric nanogenerator
Triboelectric effect
Tribovoltaic effect
Alternating-current nanogenerators
Direct-current nanogenerators

ABSTRACT

Triboelectric nanogenerators (TENGs) convert of mechanical energy into electric power, providing a simple way to low-emission, self-powering technology. Since their discovery in 2012, applications in wearable electronic devices, wave and wind energy scavenging have been discussed, but further research is required to realise the real-world application of TENGs as a clean technology. This review uniquely integrates fundamental principles, advanced design strategies, and cross-disciplinary applications, addressing critical gaps overlooked in prior studies focused on material design or single-domain applications. Specifically, we highlight the theoretical framework of displacement current incorporating triboelectric polarization; innovative charge excitation techniques enabling ultrahigh surface charge density; dual-mode (alternating-current/direct-current) operation mechanisms; and emerging applications in Internet of Things (IoT), implantable medical devices, and smart agriculture. These insights provide a comprehensive roadmap for advancing TENGs as a versatile clean energy technology.

Introduction

The rapid proliferation of Internet of Things (IoT) devices, projected to exceed 29 billion worldwide by 2030, has intensified the demand for self-sustaining energy systems, as traditional batteries face challenges in scalability, electronic waste, and carbon footprint [1,2]. Concurrently, the global transition to net-zero emissions necessitates innovative technologies for harvesting low-grade mechanical energy including human motion, wind, waves, which constitutes over 70 % of ambient energy but remains underexploited [3,4]. Triboelectric nanogenerators (TENGs), since their invention in 2012 [5], have emerged as a transformative solution, offering high power density [6], multidimensional energy harvesting capabilities, and biocompatibility [7,8], positioning them as a cornerstone for decentralized clean energy infrastructure.

TENGs are a crucial component of clean technology [5,9]. Due to advantages such as small size, light weight and high flexibility, TENGs represent a breakthrough in the field of energy harvesting and conversion, showcasing their importance in advancing clean technology [10,11]. Unlike electromagnetic generators constrained by high-frequency motion or solar cells dependent on light, TENGs uniquely address the “long tail” of mechanical energy in IoT scenarios, such as human breathing (0.1–1 Hz) [12], or ocean waves (0.01–0.5 Hz) [13]. Their flexibility, enabled by nanocomposite dielectrics, such as PDMS [14,15] and P(VDF-TrFE) [16], allows integration into textiles [17], implants [18], and even fishnets [19], overcoming the size and rigidity limitations of traditional harvesters.

When first proposed in 2012, TENG had low output power capable of only powering micro-electronic devices [5], but through material improvement and structural optimization, its power density increased from 10.4 mW m^{-3} to 31.0 MW m^{-2} by 2025 [20]. Early developments focused on low-power devices, such as self-powered sensors for human motion monitoring [21,22]. By the mid-2010s, TENGs began powering more complex systems, including implantable medical devices like symbiotic pacemakers that harvest cardiac motion energy [23,24], and flexible wearables such as silicone-based TENGs in shoes to scavenge human motion energy [25,26]. Recent years have seen expansions into environmental IoT and smart infrastructure, such as wind-driven TENGs for real-time environmental monitoring [27] and ocean energy harvesting networks for marine IoT [28,29]. In sensing, early TENGs enabled motion vector detection and tactile sensing [30,31], while later advancements introduced biomedical applications [32] and AI-driven systems [33]. Cross-disciplinary applications now span smart

* Corresponding author.
E-mail address: zhong.wang@mse.gatech.edu (Z.L. Wang).
[1] These authors contributed equally.

https://doi.org/10.1016/j.mattod.2025.06.019
Received 1 April 2025; Received in revised form 1 June 2025; Accepted 9 June 2025

agriculture [34], air purification [35], and self-powered robotics [36,37].

Nowadays, various classes of TENGs have been developed including micro-nano energy [38,39], self-powered sensing [40,41], high-voltage sources [42,43]. Applications in energy scavenging [44,45], sensors [46,47], robotics [48,49], human–machine interfaces [50,51], have been explored. and several reviews have focused on theoretical modelling [52,53], energy harvesting [54,55], self-powered sensors [56,57], and representative applications of TENGs in specific domains [57,58]. TENGs show potential applications for converting ocean energy into electric power both on the sea and underwater [59,60].

TENGs consist of three key elements: contact-electrifier, electrostatic inducor, and external circuit, as shown in Fig. 1 [61,62]. As the two dielectric material surfaces are separated, the resulting triboelectric charges drive the flow of electrons in the external circuit via electrostatic induction [63,64]. This process generates pulsed signals of alternating current [65,66]. By coupling the principles of triboelectrification and electrostatic induction, TENGs can effectively convert mechanical energy from the surrounding environment into electricity, presenting a promising solution for clean energy scavenging [67,68].

Previous reviews [69,70] have primarily focused on material engineering for enhanced charge transfer or specific applications. However, they overlook three critical gaps: (1) the fundamental theory linking triboelectrification to Maxwell's equations, (2) the systematic analysis of environmental impacts on TENG performance, and (3) the integration of DC-operation mechanisms that enable direct powering of electronics without rectifiers. This review addresses these limitations by providing a unified framework for TENG design, operation, and application, emphasizing cross-disciplinary innovations that bridge materials science, electrochemistry, and sustainable technology.

In this review, we aim to provide an in-depth overview of TENGs and their diverse applications. We begin by outlining the fundamental principles underlying TENGs, followed by an exploration of strategies to enhance their output performance. Furthermore, we introduce the wide range of applications for TENGs. Finally, we conclude with a discussion of the emerging challenges, strategies, and opportunities that lie ahead in the research and development of TENGs, highlighting the potential for future advancements in this exciting field.

Scavenging energy with TENGs

TENGs operate through a complex interplay of three primary components [61,71]. This process commences with contact electrification, during which two dissimilar materials come into contact, exchanging electrons and leading to the accumulation of static electricity, also known as triboelectrification [72,73]. The electrostatic inducer then capitalizes on the principle of electrostatic induction, inducing opposite charges on the respective surfaces of the materials [74,75]. Upon connecting an external circuit to the TENG device, the accumulated charges flow through the circuit, generating an electric current, which can be used to power small electronic devices or stored for future use [76,77]. In practical applications, TENGs employ a broad array of materials for contact electrification and electrostatic induction, including polymers such as polydimethylsiloxane (PDMS) [78,79], polytetrafluoroethylene (PTFE) [80,81], polyimide [82], as well as metals like aluminum [83] and copper [84,85]. Material selection is based on their triboelectric properties, durability, and suitability for specific applications, enabling the efficient design of TENG devices across diverse technological domains [86,87].

The principles of TENG devices

Contact-electrification (CE) is a widely observed occurrence [88]. Generally, a rubber rod rubbed with fur becomes negatively charged, while a glass rod rubbed with silk becomes positively charged [89]. However, there is still an ongoing debate regarding the underlying mechanisms of CE [90,91]. Specifically, there is a question of whether electron transfer, ion transfer, or even material species transfer is primarily responsible for driving CE [92,93]. This ongoing discussion may be attributed to the inherent limitations of measurement techniques and the complexities introduced by the frictional processes involved in CE [94,95]. It is worth noting that CE can occur across all phases of matter (solid, liquid, and gas), highlighting its fundamental nature in interfacial interactions [96,97].

Electron transfer plays a dominant role in CE [98,99]. In the context of metal-dielectric interfaces, the CE mechanism can be accurately explained using the Fermi level model for metals and the surface states model for dielectrics [100,101]. Similarly, the CE between dielectric-dielectric interfaces can be understood through the surface states model [102,103]. When two dielectric interfaces getting closer during

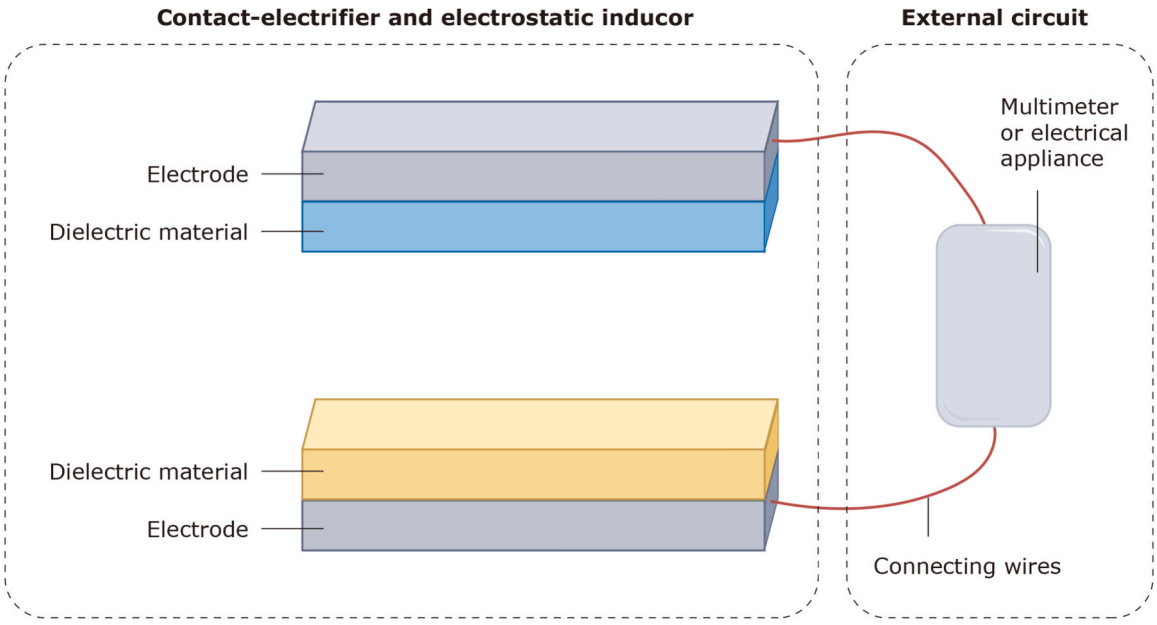

Fig. 1. Schematic structure of a typical TENG consisting of contact-electrifier, electrostatic inducor, and external circuit.

the frictional processes, CE occurs exclusively when the distance between the two materials becomes shorter than the bonding length, typically within the repulsive force region of the interaction potential between two atoms (Fig. 2) [98]. To elucidate the underlying electron transition responsible for CE, a model based on overlapped electron clouds has been proposed [104,105]. This model suggests that when two atoms experience stress, a strong overlap of their electron clouds occurs, leading to a reduction in the potential barrier between them [88,106]. As a result, electron transition from one atom to the other is facilitated [88,107]. Mechanical stressing is necessary to bring the atoms close enough to maximize the overlap of the electron clouds [108,109]. Furthermore, it is anticipated that photon emission takes place during this CE process, which has been experimentally confirmed [110,111]. For the sake of brevity and ease of reference, the electron transition model is depicted in Fig. 2c [98]. This model transcends solid–solid interfaces, offering a universal framework for comprehending CE across diverse material combinations, encompassing liquid–solid, liquid–liquid, gas–solid and gas–liquid interfaces [112,113].

CE between liquid–solid surfaces results in the formation of an electric double layer (EDL), a complex electrochemical phenomenon [114,115]. The canonical description of EDL involves the adsorption of an ion layer onto the solid surface, attracting ions of opposite charge while repelling those of the same charge in the surrounding solution [116,117]. This interaction creates an electric potential gradient near the liquid–solid interface. Wang reported a revised model for EDL formation, including two distinct steps [96,118]. Firstly, there is an electron exchange process between the liquid and solid surfaces, analogous to the electron transfer mechanisms proposed for CE. This electron exchange effectively converts surface atoms into ions. Secondly, these ions interact with the ions present in the liquid, resulting in a graded distribution of cations and anions in the vicinity of the interface. The conventional model of EDL formation had overlooked this initial electron exchange step, focusing solely on the later ion-ion interactions [119]. Nevertheless, recent experimental evidence has confirmed that electron exchange and ion adsorption occur simultaneously and coexist during liquid–solid interactions, and the formation of EDL is a result of CE at the interface [96,120]. This revised understanding of EDL formation has the potential to impact our comprehension of interface

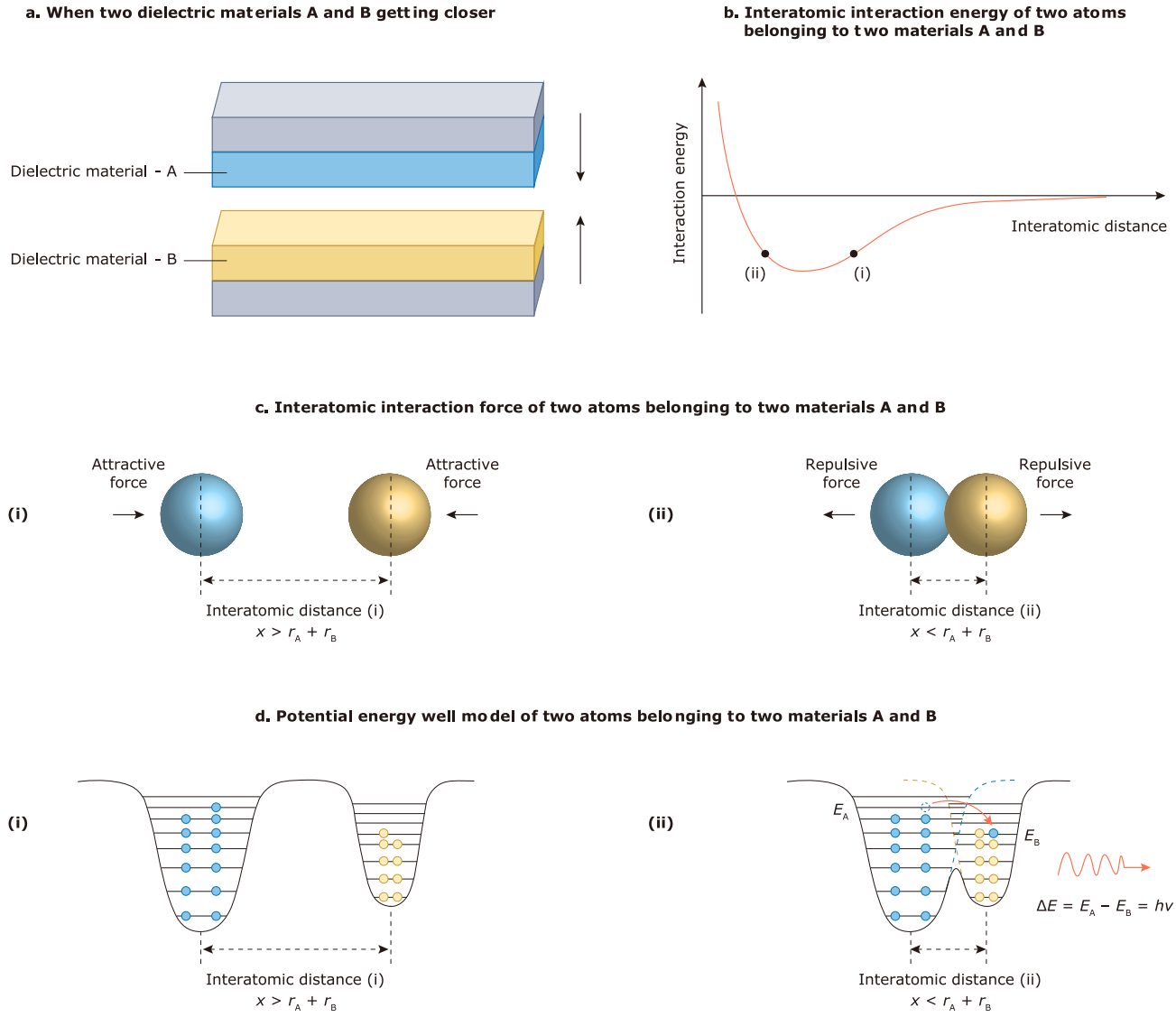

Fig. 2. The overlapped electron-cloud model proposed for explaining CE and charge transfer between two atoms for a general case. The theoretical framework for charge dynamics is supported by Maxwell's equations incorporating triboelectric polarization (see Eqs. (1)–(4) in Section "Displacement current theory"). a, When two dielectric materials A and B getting closer. b, Interatomic interaction energy of two atoms belonging to two materials A and B. c, Interatomic interaction force of two atoms belonging to two materials A and B. d, Potential energy well model of two atoms belonging to two materials A and B. Reprinted with permission [98]. Copyright 2019, Elsevier.

chemistry, electrochemistry, and even interactions at the cellular level [121].

Displacement current theory

The theoretical foundation of TENGs lies in Maxwell's displacement current, which arises from the time-varying electric field and media polarization [122]. When considering power generation in TENGs, the polarization should incorporate a component stemming from CE [123]. To appropriately account for the electrostatic charges induced by CE in Maxwell's equations, an additional term $\boldsymbol{P_s}$ was introduced in displacement vector $\boldsymbol{D}$ by Wang [124,125]:

$$\boldsymbol{D} = \varepsilon_0 \boldsymbol{E} + \boldsymbol{P} + \boldsymbol{P}_s \tag{1}$$

$$\boldsymbol{D}' = \varepsilon_0 \boldsymbol{E} + \boldsymbol{P} \tag{2}$$

The Maxwell's equations can be reformulated as a new set of self-consistent equations that were derived for moving medium/object [125–127]:

$$\nabla \cdot \mathrm{D} = \boldsymbol{\rho} \tag{3a}$$

$$\nabla \cdot \mathrm{B} = 0 \tag{3b}$$

$$\nabla \times (\boldsymbol{E} + \boldsymbol{v_r} \times \boldsymbol{B}) = -\frac{\partial}{\partial t}\boldsymbol{B} \tag{3c}$$

$$\nabla \times (\mathrm{H} - \boldsymbol{v}_r \times \mathrm{D}) = \mathrm{J} + \rho \boldsymbol{v} + \frac{\partial}{\partial t}\mathrm{D} \tag{3d}$$

where $\boldsymbol{D}$ represents the electric displacement vector field; t represents the time; $\boldsymbol{P_s}$ represents the polarization field resulting from the surface electrostatic charge; $\boldsymbol{E}$ represents the electric field strength, and ε_0 represents the vacuum permittivity; $\boldsymbol{v}$ is the translation velocity of the object; and $\boldsymbol{v_r}$ is the rotation velocity of the object. From Eq. (3d), the conduction current $\boldsymbol{J}$ can be accounted for, leading to a revised expression for the total displacement current:

$$\boldsymbol{J}_D = \frac{\partial \boldsymbol{D}'}{\partial t} + \frac{\partial \boldsymbol{P_s}}{\partial t} \tag{4}$$

Here the first term, $\frac{\partial \boldsymbol{D}'}{\partial t}$, is the displacement current arising from the temporal variation of the electric field. The second term, $\frac{\partial \boldsymbol{P_s}}{\partial t}$, corresponds to the current generated by changes in media boundaries. In the case of TENGs, the polarization field is generated through CE. The displacement current can be obtained by integrating $\boldsymbol{J_D}$ over the surface. Within the internal circuit of the TENGs, the displacement current serves as the driving force, while in the external circuit, it manifests as the conduction current. Both internal and external circuits are interconnected through electrodes, forming a complete circuit. Hence, the displacement current serves as the fundamental mechanism enabling electromechanical energy conversion in TENGs, while the conduction current represents its external expression [128].

Design of TENG devices

Maxwell's equations help to understand how TENGs turn mechanical motion into electricity: when two materials rub together, they create static charge, and moving these charged materials apart or past each other generates a changing electric field that pushes electrons through a circuit. This connection between physics principles and TENG design bridges theory and practice.

The design of TENG devices has seen developments in assessing the performance of TENGs with diverse structures and materials [129]. In 2015, Figure-of-Merits (FOMs) were initially introduced as a metric for evaluation [130]. These FOMs were derived from the operation energy output cycle, considering the built-up voltage (V) against the transferred charges (Q) [131]. Subsequently, a comprehensive performance FOM (FOM_p) was established, including both structural (FOM_S) and material (FOM_m) aspects [132]. Notably, the FOM_m is representative of the square of the surface charge density, a crucial characteristic of the materials utilized. Surface charge density plays a pivotal role in evaluating TENG performance, as power density exhibits a quadratic relationship with it [133]. Research efforts have been dedicated to enhancing surface charge density, primarily focusing on three aspects: material optimization [134,135], charge excitation [136,137], and environmental considerations [138,139].

Materials optimization

Materials optimization serves as a prevalent method in selecting appropriate triboelectric materials to improve the performance of TENGs [140]. This process heavily depends on the triboelectric series, which is established solely through mutual rubbing of two materials. This series categorizes materials based on their propensity to either lose or gain electrons, with those prone to losing electrons placed at the positive end and those prone to gaining electrons at the negative end. Notably, the traditional triboelectric series is based on empirical observations and focuses solely on charge polarity. However, in 2019, a quantified triboelectric series was introduced [141], which employed a controlled platform and environment for its establishment. This series takes into account both charge polarity and quantity, providing a valuable reference for material selection in TENGs. Nevertheless, the triboelectric performance of TENGs is still affected by the complex environment, such as gas breakdown between triboelectric layers, as well as external factors like humidity and gas molecules. As a result, the performance of TENGs remains dependent on these environmental conditions. In 2022, inspired by the integration of TENG technology with vacuum environments, a standardized methodology was introduced for evaluating the maximum triboelectric charge of dielectric materials [141]. This approach effectively overcomes the limitations posed by environmental factors and the structure of TENGs, offering a more reliable and accurate assessment of triboelectric performance. Through the evaluation of triboelectric charge density across a diverse array of over forty materials, an updated triboelectric series was formulated, providing a comprehensive understanding of the optimal triboelectric capabilities of various materials [141]. We have selected ten specific examples from these forty materials, as shown in Fig. 3, with a focus on various clean technology applications. By minimizing the impact of air breakdown and environmental influences, the vacuum triboelectric charge density measurement offers a more accurate reflection of the inherent material properties. This research emphasizes the promising direction of optimizing triboelectric behaviour by considering triboelectric material pairs, rather than focusing solely on individual dielectric materials, thereby opening new avenues for enhancing triboelectric performance.

Beyond traditional polymers, recent breakthroughs in antifreeze hydrogels and 2D nanocomposites have addressed environmental limitations. Han et al. developed a glycerol/water binary solvent dual-network gel (PASG/NaCl/Gly) with gelatin-polyacrylamide hydrogen bonding, achieving antifreeze performance at −51 °C, a surface charge density of 318 μC m^{-2} (2.4 × improvement over traditional hydrogels) [143]. Pace et al. used liquid-phase exfoliated $WS_2/WSe_2/MoS_2/Se_2$ nanosheets with PVA to fabricate electrochemical TENGs, enhancing charge storage via electrical double-layer capacitance for a peak power density of 530 mW m^{-2} (7 × improvement over pure graphene) [144].

Charge excitation

The utilization of an ultra-thin dielectric layer effectively reduces the voltage across the air gap during the separation of triboelectric layers, subsequently elevating the breakdown threshold and significantly elevating the ultimate surface charge density of TENGs. However, the limited triboelectric properties of tribo-materials, along with the intricate balance between charge accumulation and dissipation, pose

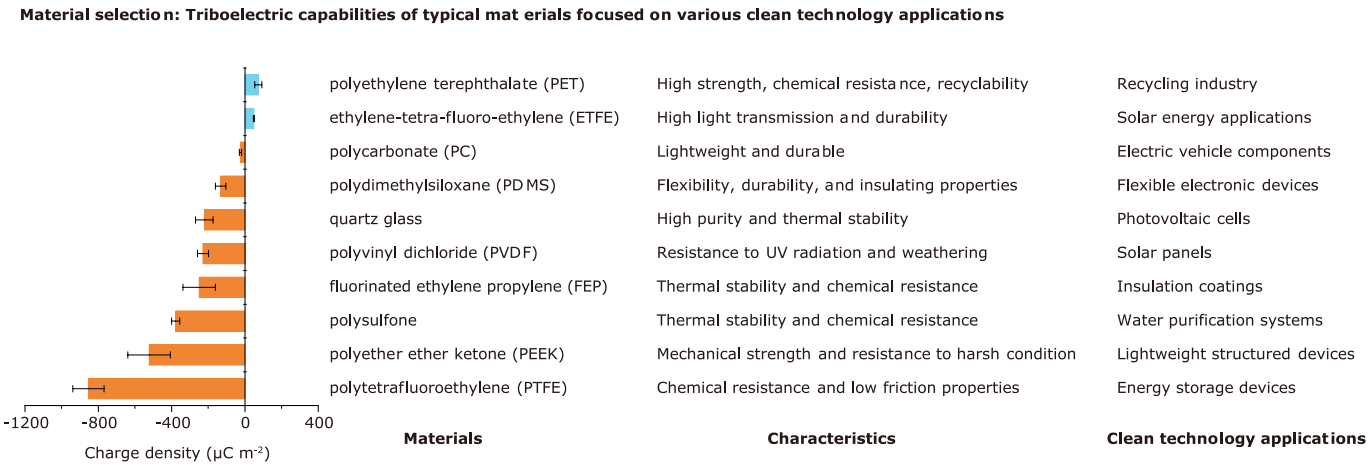

Fig. 3. The output performance of TENG optimized by material selection. Reprinted with permission [142]. Copyright 2022, Springer Nature.

significant challenges in directly achieving an optimal output through triboelectrification [145]. To overcome these limitations, charge excitation technology has emerged as a promising strategy. This approach capitalizes on the high output voltage generated by a pump TENG to efficiently charge a large capacitor as the main TENG. Consequently, the maximum output performance of TENGs becomes decoupled from the triboelectric capabilities of the involved tribo-materials, thereby opening new avenues for enhancing the efficiency and overall performance of TENGs [146].

In 2018, two independent research groups led by Wang et al. and Qin et al. made a groundbreaking discovery by introducing the first charge excitation method into TENG [147,148]. Through increasing the capacitance of the main TENG by employing thinner dielectric layers or dielectric materials exhibiting higher relative permittivity, an exceptional effective surface charge density of up to 1020 μC m^{-2} was achieved under ambient atmospheric conditions. In 2019, Liu et al. introduced two variants of the TENG: the external-charge-excitation TENG (ECE-TENG) and the self-charge-excitation TENG (SCE-TENG) by integrating a voltage multiple circuit (VMC) (Fig. 4) [149]. Remarkably, the integration of VMC allows for the substitution of the traditional parallel plate capacitor structure of TENG with commercial capacitors, thereby significantly increasing charge storage capacity and enabling the generation of elevated excitation voltages. Furthermore, this integration introduces a novel approach that facilitates the multiplication of output charge through dynamic switching of capacitor modes within the SCE-TENG, eliminating the need for additional TENGs.

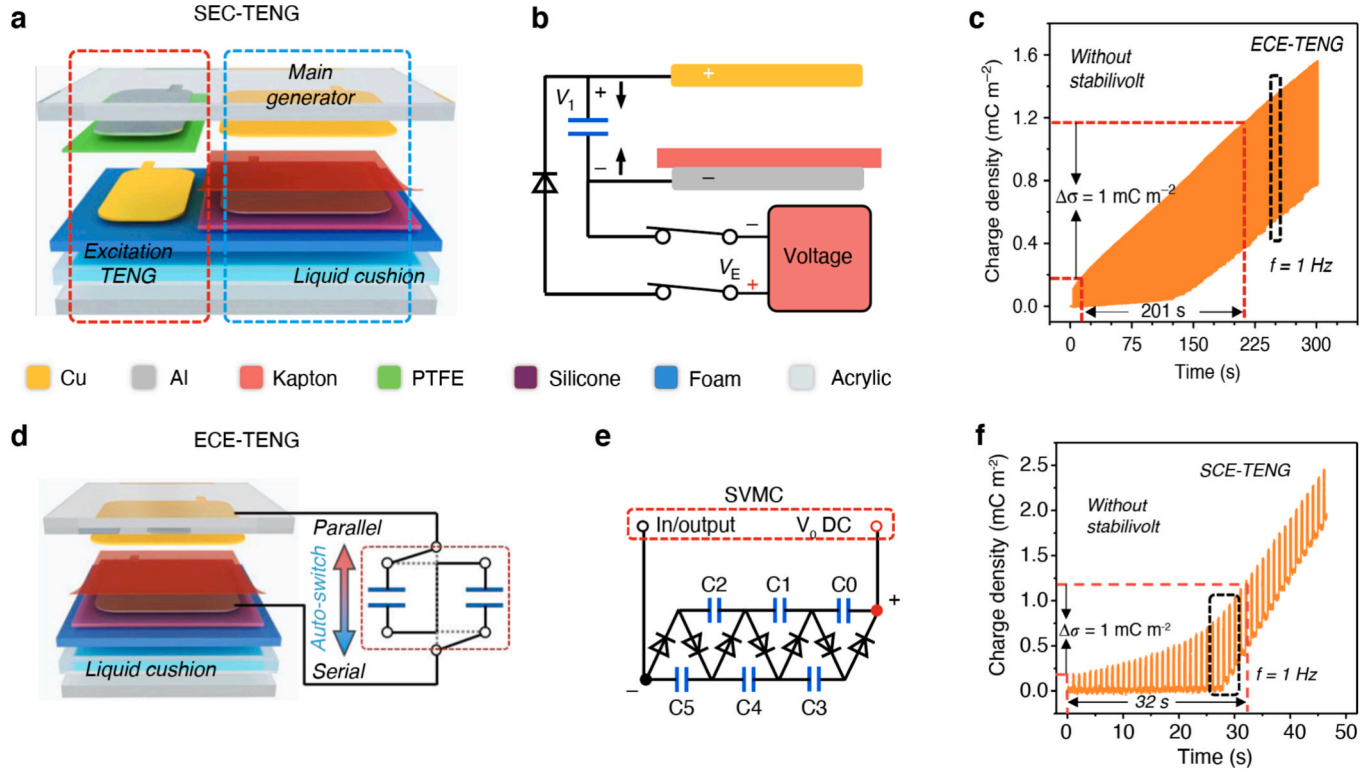

Fig. 4. Charge excitation techniques for TENG design. a, Structural illustration of ECE-TENG. b, Simplified working components of ECE-TENG. c, Dynamic output charge accumulation process of ECE-TENG. d, Fundamental scheme of SCE-TENG, the auto-switch can change capacitors from parallel to serial connection during the operation cycle. e, Input/output node and scheme of voltage-multiplying circuit. f, Dynamic output charge process of SCE-TENG. Reprinted with permission [149]. Copyright 2019, Springer Nature.

Consequently, these innovative devices have exhibited an enhancement in effective surface charge density, achieving a value of 1.25 mC m^{-2} when utilizing a 5 μm Kapton film. Furthermore, the employment of a carbon/silicone gel electrode to enhance contact efficiency led to an improvement in effective surface charge density, achieving an impressive value of 2.38 mC m^{-2} when utilizing a 4 μm polyimide (PI) film [150]. Subsequently, this metric was further elevated to 3.53 mC m^{-2} through the innovative utilization of a composite film composed of lead zirconate titanate and poly(vinylidene fluoride), exhibiting superior relative permittivity [151]. Recently, a further augmentation to 4.3 mC m^{-2} was achieved through the utilization of a carbon powder–polyvinylidene difluoride composite film [152], which stemmed from the charge trapping failure effect induced by the modulation of the carrier trap state within the dielectric film.

Recent breakthroughs in charge self-injection technology have addressed the limitations of traditional methods. Wang et al. developed an ultra-fast and high-efficiency ultra-fast charge self-injection strategy to quantify charge trapping in 30 triboelectric materials [153]. By optimizing trap distribution with nano-doping (e.g., SiO_2 and MoS_2 in P (VDF-TrFE)), they achieved a record-high retained charge density of 3.88 mC m^{-2} with a 50 % reduction in dissipation rate. This work establishes material gene banks for positive/negative charge injection, providing a standardized framework for suppressing charge de-trapping. Kuang et al. synthesized ZIF-67-D MOF with enriched (112) facets via a dual-solvent method, reducing Co coordination to 3, enhancing electron transfer, and achieving a 2.4 × increase in TENG charge density alongside 9.9×/1.9 × improvements in OER/HER electrocatalysis for self-powered water splitting [154].

Environmental control

In addition to materials optimization and charge excitation, environmental considerations have emerged as a critical strategy for enhancing the performance of TENG devices. Given the sensitivity of TENGs to environmental factors such as atmospheric pressure, humidity, and temperature, efforts have been directed towards creating controlled environments that minimize these influences. Encapsulation techniques, such as the use of protective coatings and barrier materials, have been explored to shield TENGs from external elements [155]. Moreover, the development of specialized housing or packaging for TENG devices has been investigated to maintain stable operating conditions and prolong device lifespan [156].

Typically, the separation of the triboelectric layers generates a robust electrostatic field within the air gap between them. However, this process is accompanied by the loss of surface charges caused by air breakdown. To mitigate the loss of charges due to air breakdown, researchers have successfully created a high vacuum environment. This approach effectively restrains the air breakdown effect, leading to a significant increase in charge density [157]. Additionally, Zi et al. conducted an in-depth study on the performance of TENG across varying atmospheric pressures [158]. Their findings reveal that in environments with high atmospheric pressure, the charge density is significantly enhanced due to the suppression of the air breakdown effect [158]. Humidity plays a pivotal role in modifying surface conditions, which subsequently impacts the behavior of charge transfer. This modulation can result in an improvement of surface conductivity, ultimately promoting the rate of charge loss. Notably, the process of air breakdown is also influenced by varying humidity conditions, undergoing modulation accordingly. Previous investigations have revealed a tendency for the output charge density to decrease as humidity increases, suggesting that optimal performance is attainable in drier environments [159].

Recently, Liu et al. have elucidated that in environments of high humidity, ions exhibit greater stability on the dielectric surface compared to electrons [160]. Consequently, TENGs that possess a significant preponderance of ions on their surface demonstrate superior and more consistent output performance in comparison to those primarily composed of electrons. Elevating temperature can facilitate the dissipation of surface charges due to the thermionic emission effect, which may impact the output performance of TENGs. However, contrary to this intuitive understanding, several studies have revealed that increasing the temperature gradient across the triboelectric layers in contact actually enhance the output charge density. In 2019, Lin et al. utilized atomic force microscopy (AFM) and Kelvin probe force microscopy (KPFM) techniques to demonstrate that, at the nanoscale, a hotter solid preferentially acquires positive triboelectric charges, whereas a cooler solid inclines towards acquiring negative charges, particularly in metal-inorganic triboelectric material pairs [161]. This research highlighted that the transferred charge density between two solid materials can be modulated by adjusting the temperature difference. Building upon this foundation, a macroscopic experiment conducted in 2021, involving metal–organic triboelectric material pairs, further validated these observations [162]. Notably, as the temperature difference increased from 0 K to 145 K, the surface charge density rose threefold, offering a promising approach to elevate the output performance of TENGs in high-temperature operational environments. Xia et al. used Zr-Cu-Al MG for low-friction (coefficient 0.05, 60 % reduction vs. Cu), high charge density (330 μC m^{-2}), and operation near the theoretical breakdown limit under 0.75 atm pressure, achieving a peak power density of 15 MW m^{-2} to power 9 W LEDs [163].

To quantitatively assess the efficacy of these strategies, Table 1 summarizes representative approaches for enhancing TENG performance, highlighting their key metrics, environmental adaptability, and limitations. Actually, TENG device design is a comprehensive issue. The design of TENG devices encompasses not only material optimization, charge excitation, and environmental considerations, but also necessitates attention to structural design, mechanical design, integration and system design, as well as safety and compliance. This involves determining the structure and configuration of the TENG device, encompassing the arrangement of the triboelectric layers, electrodes, and the overall device geometry. Factors such as flexibility, scalability, and ease of manufacturing must be taken into account. Additionally, the mechanical aspects of the device need to be considered, including the method of triggering or activation, the movement of the triboelectric layers, and the overall mechanical robustness. Integration of the TENG device into the intended system or application is crucial to ensure compatibility and functionality within the larger framework. Furthermore, adherence to safety standards and regulatory requirements is essential, particularly if the device will be utilized in consumer products or industrial settings.

Operation of TENG devices

TENGs exhibit seven distinct operational modes tailored to diverse mechanical energy sources and application scenarios (Fig. 5a). Among these, five are alternating current (AC) modes based on triboelectrification and electrostatic induction, while two are direct current (DC) modes enabled by novel charge transfer mechanisms.

On the basis of the principles of triboelectrification and electrostatic induction, the traditional TENG has the capability to convert mechanical energy into AC electricity, commonly referred to as AC-TENG. Taking into account various mechanical motions, five fundamental working modes have been established for the AC-TENG [164,165], enabling it to harvest diverse forms of energy. These modes include: (i) Vertical contact-separation mode (CS-mode), where two triboelectric layers alternately come into contact and separate vertically, leading to variations in charge transfer and potential difference based on the separation distance. Periodic vertical motion between triboelectric layers generates alternating current, widely used in wearable tactile sensing [166]. (ii) Lateral sliding mode (LS-mode), involving the relative lateral movement of the triboelectric layers along a tangential direction, resulting in changes in charge transfer and potential difference as a function of sliding displacement, which leverages tangential displacement for harvesting environmental mechanical energy [167]. (iii) Single-electrode

Table 1
Performance comparison of TENG enhancement strategies.

Strategy	Example/Technique	Surface Charge Density	Power Density	Environmental Adaptation	Key Limitations	Ref.
Charge Excitation	DC-TENG with mismatched triboelectric units and electrodes	N/A	33.20 mW (at 80 MΩ)	Marine environment (saltwater corrosion protection)	Dependent on rotational speed for output stability	[129]
Material Optimization	Selection of triboelectric material pairs (TPU-ETFE) for DC-TENG	241.6 nC	N/A	Ambient atmospheric conditions	Limited by air breakdown in charge transfer	[133]
Charge Excitation	External charge excitation (ECEF-TENG) with dielectric oil and self-voltage-multiplying circuit (SCEF-TENG)	260.15 μC m^{-2} (ECEF) and 212.5 μC m^{-2} (SCEF)	16.28 mW (ECEF)	High dielectric strength oil for stable charge storage	Reliant on high-voltage stability and oil durability	[136]
Charge Excitation	Integration of charge excitation circuit with TENG network	N/A	25.8 mW (single TENG), 24.6 mW (network)	Marine environment (water wave energy harvesting)	Dependent on wave frequency/amplitude, circuit complexity	[137]
Environmental Control	Studying effects of relative humidity and pressure on TENG performance	~50 nC	N/A	Varying RH (10–90 %) and pressure (50 Torr–atmospheric)	Charge stability affected by environmental fluctuations	[138]
Material Optimization	Standardized measurement of triboelectric charge density (TECD) using liquid metal (mercury) as reference	−148.20 μC m^{-2} (Viton fluoroelastomer rubber)	N/A	Controlled N_2 environment (20 ± 1°C, 0.43 % RH)	Sample surface cleanliness and environmental stability requirements	[141]
Material Optimization	Standardized measurement of intrinsic triboelectric charge density (σ_t) in vacuum using contact-separation TENG	1250 μC m^{-2} (PVC-Cu)	N/A	High vacuum environment (5 × 10^{-5} Pa, 298 K)	High vacuum requirement, material transfer effects	[142]
Material Optimization	Development of PASG/NaCl/Gly dual-network gel with antifreeze and self-adhesive properties	N/A	462 mW m^{-2} (gel-TENG)	−51 °C (antifreeze capability)	Limited conductivity at extremely low temperatures	[143]
Material Optimization	Integration of 2D transition metal dichalcogenides (TMDs) in PVA gel electrolyte for FLG electrodes	N/A	530 mW m^{-2}	Ambient conditions (humidity ~ 40 %, 20–21 °C)	Stability affected by gel leakage in wet encapsulation	[144]
Charge Excitation	Triboelectrification Enhancement Effect (TEE) via dynamic contact for charge saturation	Up to 2.2 mC (transferred charge)	20.6 W m^{-2}	Ambient conditions (humidity 30–90 %, temperature 20–40 °C)	Performance decay over time due to charge escape	[145]
Charge Excitation	Polytetrafluoroethylene (PTFE) powder forming film (PPF) with PU foam for enhanced contact efficiency	Up to 945 μC m^{-2}	8.32 W m^{-2}	High humidity (85 % RH)	Powder aggregation over time affecting contact efficiency	[146]
Charge Excitation	Self-Charge-Pumping TENG (SCP-TENG) with floating layer structure	1020 μC m^{-2}	19.8 W m^{-2}	Ambient conditions (room temperature/humidity)	Charge dissipation over time	[147]
Charge Excitation	Self-Improving Triboelectric Nanogenerator (SI-TENG) with planar-parallel capacitor structure (PPCS)	490 μC m^{-2}	N/A	Ambient air environment	Charge dissipation over time affecting long-term stability	[148]
Charge Excitation	Integrated Self-Charge Excitation Triboelectric Nanogenerator (SCE-TENG) with voltage-multiplying circuits (VMC/SVMC)	1.25 mC m^{-2}	38.2 W m^{-2}	Ambient conditions (humidity ≤ 50 %)	Complex circuit design affecting device compactness	[149]
Charge Excitation	Charge-Excitation Triboelectric Nanogenerator (CE-TENG) with carbon/silicone gel electrode for enhanced contact efficiency	2.38 mC m^{-2}	115.6 W m^{-2}	Low humidity (5 % RH)	Sensitivity to humidity changes affecting air breakdown	[150]
Charge Excitation	Charge-Excitation TENG (CE-TENG) with PZT-PVDF composite film and self-polarization effect	3.53 mC m^{-2}	142.5 W m^{-2}	Low humidity (5 % RH)	Polarization decay over time in intermittent operation	[151]
Charge Excitation	Charge Trapping Failure Effect in CE-TENG with Carbon Powder-PVDF Composite Film	4.13 mC m^{-2}	58.2 W m^{-2} Hz^{-1}	Low humidity (5 % RH)	Conductivity mismatch affecting long-term stability	[152]
Charge Excitation	Ultra-Fast and High-Efficiency Charge Self-Injection (UH-CSI) with Trap State Regulation	26.2 mC m^{-2}	41.67 W m^{-2} Hz^{-1}	Low humidity (5 % RH)	Charge dissipation due to shallow traps and air breakdown	[153]
Environmental Control	Three-dimensional electrode structure with FEP pellets in encapsulated TENG units	N/A	8.69 W m^{-3} (ideal agitations), 2.05 W m^{-3} (water waves)	Marine environment (water waves)	Structural complexity affecting scalability	[155]
Environmental Control	Desiccant-based TENG (D-TENG) with honeycomb-structured paperboard frame and PTFE/Cu triboelectric layers	N/A	0.7 mW (peak power at 500 MΩ)	Packaging environment (humidity-sensitive)	Moisture absorption affecting charge retention	[156]
Environmental Control	High vacuum operation (P ~ 10^{-6} torr) combined with ferroelectric BT material for enhanced charge density	1003 μC m^{-2}	20 W m^{-2}	High vacuum environment	Dielectric breakdown limitation (~1115 μC m^{-2})	[157]
Environmental Control	High-pressure gas environment (up to 10 atm) to suppress air breakdown	Up to 558.7 μC m^{-2} (CS mode)	664 W m^{-3} (CS mode at 7.69 atm)	High-pressure gas environments (e.g., deep ocean)	High-pressure gas environment (up to 10 atm) to suppress air breakdown	[158]
Environmental Control	Utilizing optimal relative humidity (RH) to form water bridges between triboelectric materials	N/A	N/A	Humidity-controlled environments (28–35 % RH for most pairs)	Limited to specific humidity range; water film formation at high RH	[159]

(*continued on next page*)

Table 1 (*continued*)

Strategy	Example/Technique	Surface Charge Density	Power Density	Environmental Adaptation	Key Limitations	Ref.
Environmental Control	Hydrophobic PTFE dielectric with ion injection for high humidity resistance	167 μC m^{-2} (after 4500 cycles at 90 % RH)	664 W m^{-3} (at 7.69 atm)	High humidity (up to 90 % RH)	Ionic charge stability limit; material cost	[160]
Environmental Control	Temperature difference-induced electron transfer via thermionic emission in metal-dielectric contact	N/A	N/A	Variable temperature conditions	Local temperature uniformity control	[161]
Environmental Control	Temperature difference triboelectric nanogenerator (TDNG) leveraging thermionic emission and charge transfer	58.8 μC m^{-2} (optimal $\Delta T = 145$ K)	206.7 μW (at 3 MΩ)	High-temperature environments with temperature gradients	Thermal management complexity; material degradation at extreme temperatures	[162]

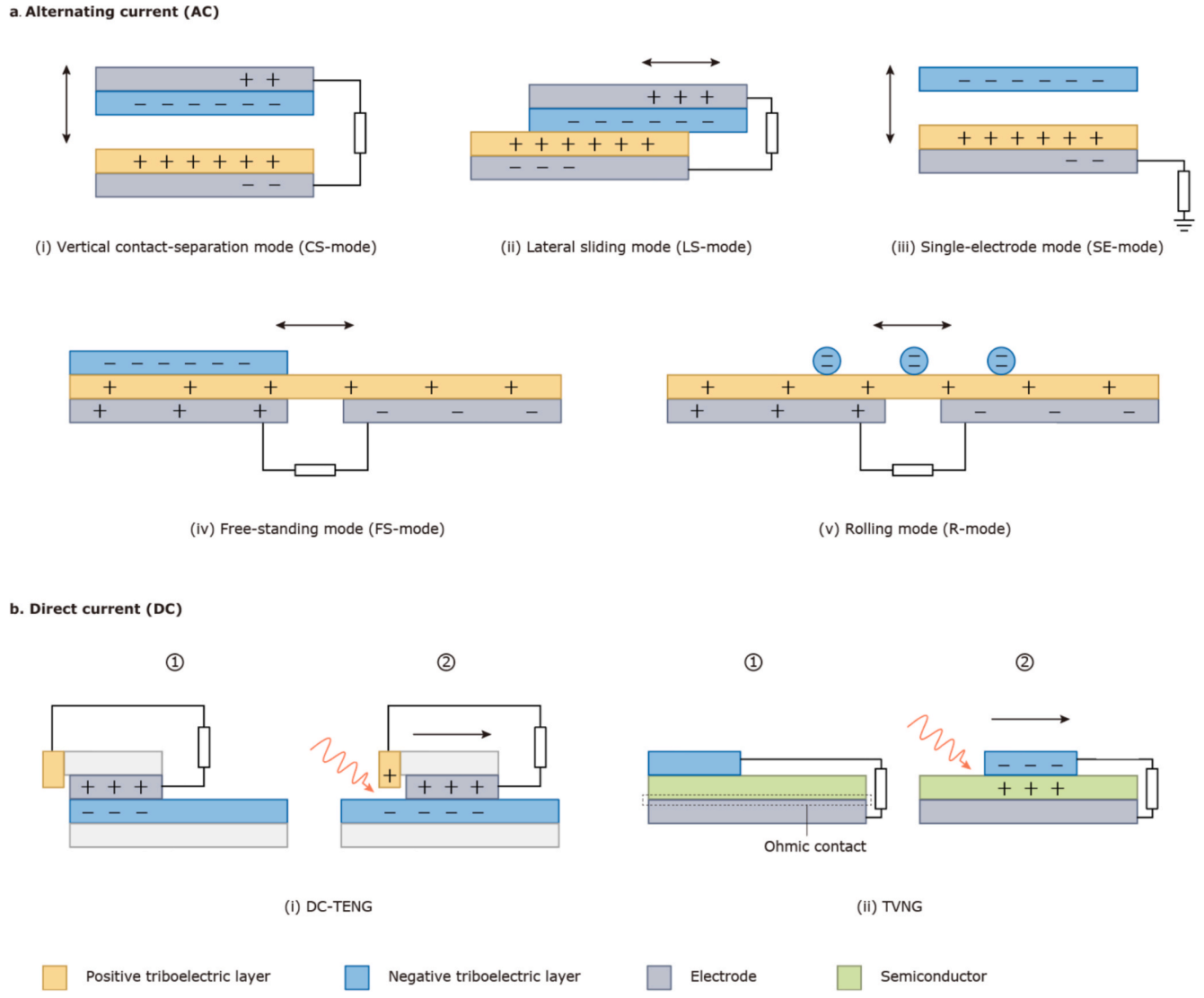

Fig. 5. The work modes of TENG. a, AC modes rely on time-varying triboelectric polarization P_s, as described by the displacement current theory in Eq. (4). **b**, DC modes enable unidirectional charge transfer, supported by Maxwell's equations for moving media (Eqs. (3c) and (3d)).

mode (SE-mode), designed to address the inconvenience of connecting both ends of the relative motion in daily applications. In this mode, only the static end of the TENG is connected to the ground through electrical loads in external circuits, leading to variations in charge transfer and potential difference relative to the ground based on the contact area. This mode enables simplified integration into IoT sensors by grounding one electrode [168]. (iv) Free-standing mode (FS-mode), where the moving part comprises either a dielectric or conductive layer, while the static part consists of symmetrically arranged electrodes. The charge transfer and potential difference between the electrodes vary according to differences in contact area. This mode is ideal for harvesting energy from human motion [169]. (v) Rolling mode (R-mode), which primarily relies on the rolling CE between spheres and a solid surface. By designing the electrodes beneath these rolling elements, power output is generated due to the disrupted charge equilibrium caused by the rolling motion. This mode effectively reduces material wear during triboelectrification

while maintaining high output performance, showing notably potential in blue energy harvesters [170].

Triboelectric charge, always harvestable through electrostatic induction, often suffers from significant losses due to electrostatic breakdown. To address this challenge and harness the energy released during breakdown, a next-generation (DC-TENG) is designed via the triboelectrification effect and induced artificial lightning [171]. The DC-TENG employs a frictional electrode that interacts with a dielectric triboelectric layer, generating a quasi-permanent charge (Fig. 5b, i). As the slider is moved, a robust electric field is established between the charge-collecting electrode and the dielectric film, leading to ionization and subsequent electron transfer. This process completes an electric loop, enabling a continuous DC output. The DC-TENG functions as both an electric charge source and a capacitor with a breakdown mechanism. It can consistently produce a current output as long as the charge source supplies sufficient charges for air breakdown. Notably, this device has demonstrated the ability to directly power electronic devices without the need for a rectifier or energy storage unit via structural design: Forward sliding creates a high electrostatic field between the charge-collecting electrode and triboelectric layer, inducing air breakdown for unidirectional charge transfer. Reverse motion lacks sufficient field strength, preventing reverse current. For example, Zhang et al. demonstrated a high-voltage-applicable DC-TENG for efficient self-powered air purification, offering potential way to enhance indoor air quality for human health protection [172].

DC-TENG offers distinct advantages in its direct current characteristics, enabling the direct driving of electronics without the need for rectifiers or energy storage devices. This capability holds great promise for practical applications and is particularly important for advancing the miniaturization of IoTs and self-powered systems. Furthermore, exploring novel principles that enable DC output is essential for expanding our understanding of TENG from new perspectives. The tribovoltaic nanogenerator (TVNG) [173], leveraging dynamic semiconductor interfaces, produces DC output through a mechanism distinct from that of TENG (Fig. 5b, ii). This process begins with the contact of stationary metal sliders with semiconductors under pressure, resulting in electron flow due to Fermi energy differences. This flow creates charged surfaces and an electric field at the interface. As the metal slides, friction energy excites carriers, driving electron flow from the semiconductor to the metal, thus generating a positive current and voltage in the external circuit. When the metal ceases movement, both current and voltage drop to zero. Conversely, sliding in the opposite direction maintains the electric field and carrier motion, resulting in a continued positive current and voltage. In essence, the TVNG leverages the properties of semiconductors to generate a DC signal during the sliding process. The performance and functionality of TVNGs depend on the design and optimization of dynamic semiconductor interfaces [174]. Future advancements in interface engineering could enable multifunctional TVNGs capable of simultaneous energy harvesting and sensing [175].

In brief, the operation of TENG devices involves the conversion of mechanical energy into electrical energy through the process of triboelectrification and electrostatic induction. When two dissimilar materials contact or displace, a potential difference is generated, leading to the flow of electrons and the generation of electricity. This section provides an illustration of the five modes for AC TENGs and the two modes for DC TENGs, each tailored to different operational requirements based on diverse structures. These distinctive processes empower TENG devices to capture energy from a range of mechanical movements, rendering them versatile for numerous practical applications.

Applications of TENG technology

The applications of TENG technology have expanded, marking key milestones in the field and drawing from the results of diverse research groups. This section aims to explore the wide-ranging applications of TENG especially in clean technology, highlighting the pivotal contributions and breakthroughs achieved by various research endeavors. From advancements in energy harvesting to the integration of TENGs in self-powered systems and beyond, the collaborative efforts of research groups have propelled the practical implementation of TENG technology across diverse domains. This section will delve into the impactful applications of TENGs, showcasing the transformative potential of this technology in real-world scenarios.

Wind energy scavengeing

The TENGs have been extensively used to scavenge wind energy [176,177]. They offer numerous advantages over traditional wind turbines, including ease of implementation, versatility in application, safety, and environmental benefits [178,179]. Compared to conventional wind turbines, TENG is simpler to implement, requiring no large structures or complex installation processes. It can be deployed in densely populated areas as a portable power source for small electronic devices, environmental monitoring, and sensor networks, without the need for open or flat spaces. In contrast to conventional wind turbines, TENG does not present safety concerns, as it operates quietly and has minimal impact on the ecosystem. Recent advancements have significantly improved the lifespan and power output performance of TENG through the use of new materials and enhancement strategies [180,181]. Key material strategies include antifreeze hydrogels and 2D nanocomposites, optimizing charge generation for low-frequency wind [143,144]. Furthermore, TENG can function as an alternative power source to traditional lithium-based batteries, reducing environmental impact and providing ecological benefits [182,183].

TENGs can convert wind energy into electricity for various applications, including powering sensors [184,185], air purification [186,187], and industrial monitoring [188]. They can also function as sensors themselves, detecting wind speed, direction, and other environmental data [189]. Additionally, wind scavenging TENGs are used for corrosion protection [190], electrolysis [191], and energy recycling [192], showcasing their versatility in harsh environments. In 2013, the first TENG-based wind harvester has been invented by Yang and his coworkers [41]. A typical TENG-based wind harvester is based on a vibration film fixed with the two ends between two electrodes [193], allowing for contact and separation induced by the wind. Such motion generates output signals. Moreover, various structures have been developed for enhancing the output performances of TENG-based wind energy harvesters [194]. Wang et al. reported that the hybrid between the solar and wind energy scavenging can be well realized by integrating the conventional solar cells and the TENG-based wind harvesters [195], which has the potential applications in smart cites, as shown in Fig. 6a. This hybrid system combines solar cells' high-frequency photon conversion with TENGs' low-frequency wind energy harvesting, demonstrating complementary energy capture for continuous power supply in smart infrastructure. The TENG-based wind energy harvester can be also used in smart agriculture [196], where the device can scavenge wind energy to improve agricultural production as shown Fig. 6b. Compared to traditional wind energy harvesters, the TENG-based wind energy harvesters will have more advantages including lower cost, larger wind scavenging range, and no rotation parts. Superhydrophobic coatings enhance outdoor durability by reducing biofouling [19,85]. The advantages can push the fast development of TENG-based wind energy harvesters in the fields, where the conventional wind energy harvesters can not be used such as in cities, in nature reserves and so on. Moreover, the performance improvements are still needed for the TENG-based wind energy harvesters including new materials, new structures, and device integration methods. Structural materials like metallic glass demonstrate mechanical-chemical co-optimization for high-efficiency energy conversion [163].

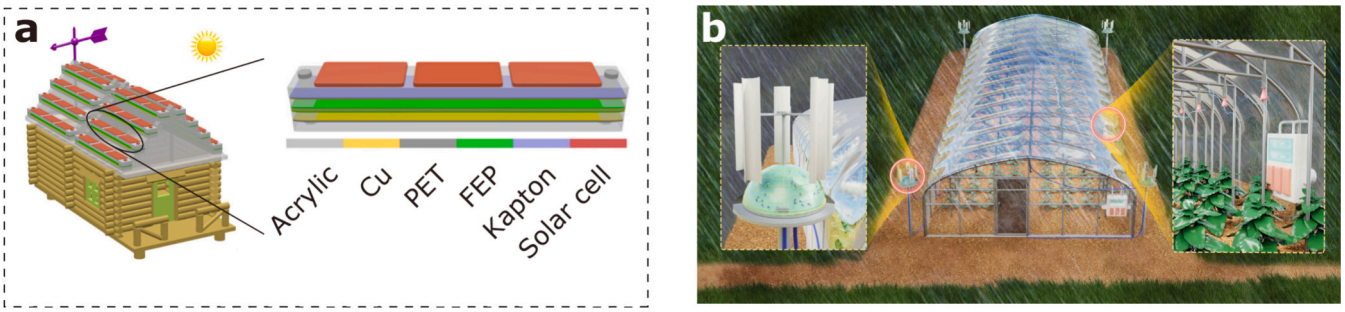

Fig. 6. Wind energy scavenging. a, Smart city. Reprinted with permission [195]. Copyright 2016, ACS Publications. b, Smart agriculture. Reprinted with permission [196]. Copyright 2022, Springer Nature.

Wave energy scavengeing

The blue energy as one key technique of TENGs can scavenge wave energy on the surface of ocean, as shown in Fig. 7. The first TENG-based blue energy harvester was reported in 2013 by Yang et al. [59], where the wave excitation can drive a plastic ball to contact and separate the inner wall of a spherical shell for producing the electricity. Prof. Wang proposed a blue energy dream [197], which is based on millions of spherical balls of TENGs connected by fishing nets to harvest wave energy. By exploiting the contact and separation between the dielectric material ball and electrodes within a dielectric hollow sphere, electric output signals can be induced.The obtained electricity from hundreds of TENGs have been demonstrated to produce hydrogen fuel [198], and power navigation systems [199]. By using the interaction of two quasi-symmetrical domains to obtain the double charge output, an ultrahigh charge density of 1.85 m C m^{-2} can be achieved for water wave energy harvesting [200].

To address the energy demands inherent in utilizing TENG technology in fishing nets, various factors need to be considered, including the typical energy requirements of fishing operations such as lighting, communication equipment, and potentially even small-scale refrigeration for preserving the catch. Current TENG devices are capable of directly harvesting energy from mechanical motion, or they can be integrated into nets or associated fishing equipment to capture energy from these movements, thereby enhancing the scalability of TENG devices to meet the energy demands of the application. This enhances the scalability of TENG devices to meet the energy demands of the application. However, several challenges must be addressed when implementing TENG in fish net applications. These include ensuring the durability and reliability of TENG devices in the harsh marine environment, understanding the impact of water exposure on performance, and mitigating the potential effects of biofouling or debris accumulation on TENG efficiency. Materials like PTFE in TENGs reduce microbial adhesion via low surface energy (contact angle = 114°), while $Gd(OH)_3$/TPU-MXene-$Gd(OH)_3$/TPU films achieve superhydrophobicity (contact angle = 150°) through $Gd(OH)_3$/TPU nanofibers, delaying biofilm

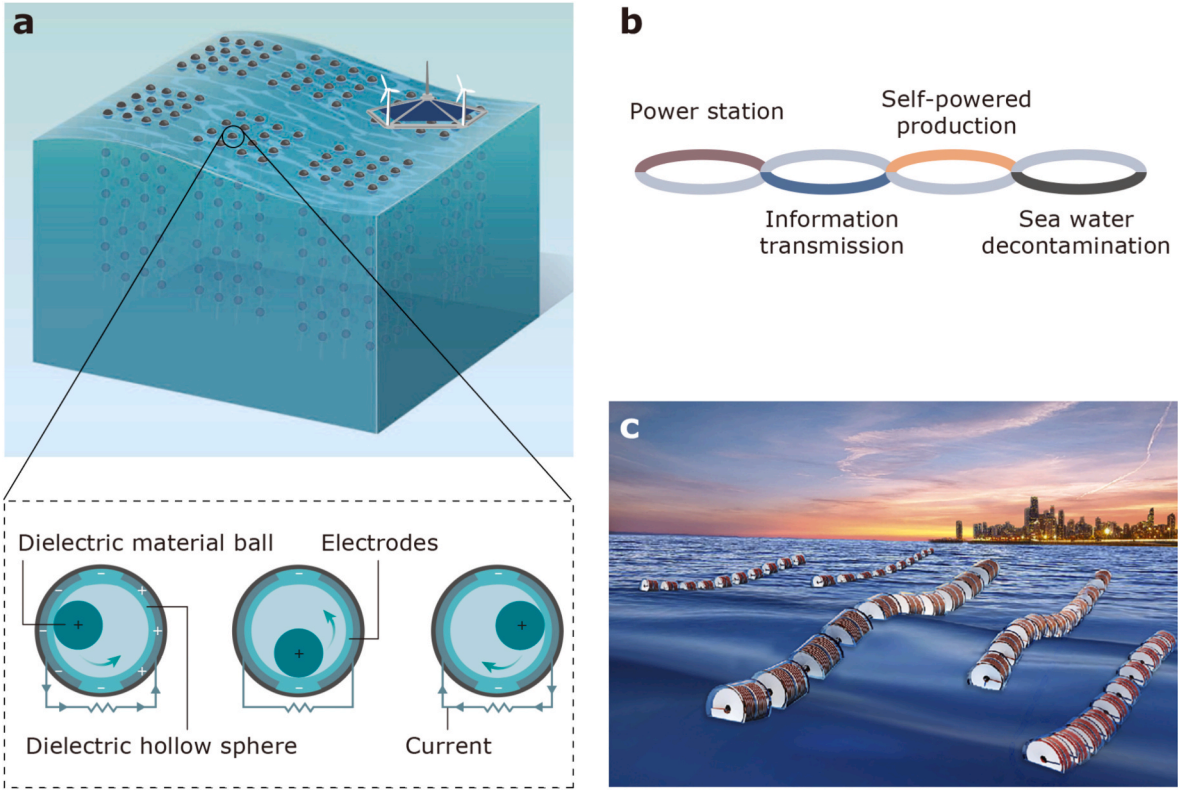

Fig. 7. Wave energy scavenging. a, Floating nets of nanogenerators to scavenge renewable wave energy. Reprinted with permission [197]. Copyright 2017, Springer Nature. b, TENGs' applications for deployment at sea. c, TENG-based wave energy harvester using a anaconda-shaped spiral multi-layered structure. Reprinted with permission [205]. Copyright 2021, Cell Press.

formation [19,85]. Saltwater corrosion of electrodes poses a critical threat to long-term performance, while TENG-driven cathodic protection reduces corrosion rates by 90 % [190]. Additionally, the integration of TENG devices with existing fishing gear should consider factors such as added weight, flexibility, and maintenance requirements.

Zhang et al. reported an active resonance TENG that can harvest omnidirectional and frequency varying wave energy, showing the potential applications in large-scale blue energy harvesting [45]. In 2018, the sea snake structure-based TENG can deliver an output peak power density of 7 W m^{-3} [201]. A tower-like structure-based TENG was reported to have the peak power density of 10.3 W m^{-3} [202]. Moreover, the multi-layered structures have been utilized to enhance the output peak power density up to 15.3 W m^{-3} [203]. The output peak power density of TENG can be enhanced to 200 W m^{-3} by using the bifilar-pendulum-assisted multi-layered structures [204]. A anaconda-shaped spiral multi-layered TENG can deliver a peak power density of 347 W m^{-3} [205], which is largest peak power density for blue energy scavenging. Currently, the largest power density of TENG-based wave energy harvester can be up to 347 W m^{-3} via using a anaconda-shaped spiral multi-layered structure [205]. Wang et al. developed a rolling-mode TENG with multi-tunnel grating electrodes and opposite-charge enhancement for efficient wave energy harvesting [170]. The device achieves an instantaneous power density of 185.4 W m^{-3} Hz^{-1} and powers a self-powered ocean sensing system with 0.8 km wireless communication capability. By integrating stacked devices and a power management module, the rolling-mode TENG demonstrates scalability for marine IoT applications, addressing the challenge of low-frequency energy harvesting in harsh environments. Future developments may integrate TENGs with flexible solar panels or ocean thermal energy conversion systems to create hybrid marine energy networks. For example, floating TENG-wave devices paired with solar panels have shown potential for self-powered marine IoT via dual energy scavenging [28].

More new materials and structures will be developed to enhance the performances of TENG-based wave energy harvesters. We believe this new technique will have a large contribution for renewable energy scavenging in the world in future. As compared with the conventional solar or wind energy, an obvious advantage of wave energy is the stability due to the corresponding mechanism. Moreover, the surface area of the ocean is enormous, suggesting the potential applications of wave energy harvesters in ocean-related fields.

Wearable sensors

In the realm of wearable sensors, TENGs offer a myriad of advantages, aligning with the principles of clean technology. These advantages include self-sustaining energy generation, reduced reliance on traditional batteries, and environmental friendliness. TENG technology excels in capturing ambient mechanical energy from human motion and other natural activities, providing a continuous power source for wearable sensors without the need for disposable batteries. This not only reduces electronic waste but also aligns with sustainable and eco-friendly objectives. Additionally, TENG's capacity to autonomously power wearable sensors contributes to the overall reduction of carbon emissions associated with traditional battery production and disposal. By seamlessly integrating with wearable sensor technology, TENG enables self-sufficient energy production, thereby advancing the progress of clean technology in the field of wearable sensors.

TENGs have been used to power various wearable electronic devices. Peng and the coworkers introduced a TENG-based electronic skin capable of monitoring human physiological signals and joint motions [206]. This system utilized silver nanowires positioned between polyvinyl alcohol and polylactic-co-glycolic acid as the TENG components. Dong et al. developed a TENG-based 3D e-textile serves as a multifunctional pressure sensor for human motion monitoring and a self-powered identification carpet [207]. The 3D e-textile's layered architecture, with interlaced triboelectric and conductive yarns, enables simultaneous pressure sensing and energy harvesting, demonstrating how spatial arrangement of materials enhances multifunctionality. Moreover, TENGs have been utilized as self-powered motion vector sensors [208], where it consists of a mover of a polytetrafluoroethylene film coated with an array of Cu electrodes and a stator of a polyimide film with the both surfaces coated with an array of Cu electrodes. Wang et al. repored a silicone based TENG, which was placed inside shoes to scavenge human-induced movement energy for powering some wearable electronic devices [209], where a high surface charge density of 250 μCm^{-2} can be obtained. A power management circuit has been used to convert radom AC energy produced by TENG to DC electricity with a efficiency of about 60 % [210], where this power unit can deliver a continuous DC electricity of 1.044 mW for powering some wereable electric devices. By integrating the TENGs with the other energy harvesting units, the hybrid energy cells can provide multi energy scavenging types to realize the stability of energies. Wen et al. reported a hybrid energy cell consisting of the fiber-shaped dye-sensitized solar cells and fiber-shaped triboelectric nanogenerators [211], which can simultaneously harvest outdoor solar energy and random body motion energies. Chen et al. reported a textile-based hybrid energy cell [39], which can charge a 2 mF capacitor to 2 V in 1 min under both the ambient sunlight and mechanical excitation.

TENGs have gained significant attention and have been widely employed in various wearable electronic devices (Fig. 8). For instance, Guo et al. developed a TENG-based auditory sensor, which proved to be beneficial for external hearing aids in intelligent robotic applications [212]. TENGs have been used to monitor the heat impact to assist in clinical analysis and prevention of mild concussions [213]. By integrating TENGs with a wearable glass, an active eye tracking system can monitor eye movements for realizing the potential applications in virtual reality, human–computer interaction, and medical monitoring [214]. In eye-tracking wearables, the integration of TENGs with flexible glass substrates requires precise alignment of microelectrodesto detect subtle ocular motions, highlighting the importance of mechanical compliance and spatial precision. In a notable development, Lu et al. reported a wearable TENG-based lip-language decoding system [215], achieving a test accuracy of 94.5 % when training 20 classes with 100 samples each. Another interesting application involved Fan et al., who fabricated a wearable TENG-based all-textile sensor array for monitoring the arterial pulse waves and respiratory signals [216], demonstrating the potential applications in personal health management. Zhu et al. developed a wearable TENG-based bidirectional sensor capable of monitoring the movements of all the joints in the human upper limbs [217], showing the potential applications in robotic automation, healthcare, and training. a TENG and electromagnetic generator-based electronic watch can be self-powered by harnessing motion energies from the wearer's wrist [218]. After charging a 100 μF capacitor for 39 s, this watch can operate for 456 s. A wearable TENG-based tactile sensor has been used to identify different materiadue to contact-induced electrification [219]. A TENG-based shoes have been fabricated to harvest human biomechanical energy to power some conventional electronics including thermometers, wearable watches, and pedometers [210].

While TENG applications in wind/wave energy harvesting and wearable electronics share foundational principles, their operational demands and environmental challenges differ significantly. Both face environmental sensitivity: marine TENGs combat saltwater corrosion and biofouling [85,190], while wearables address sweat-induced charge dissipation and mechanical wear [145,159]. In energy management, wind/wave systems require large-scale storage for intermittent low-frequency motion [13,195]. Wearables, conversely, rely on miniaturized circuits, e.g., shoe TENGs using 60 % efficient AC-DC conversion to power devices [210]. Scalability challenges also diverge: ocean-wide wave harvesting networks [197] demand cost-effective materials, while wearables prioritize compactness [220] with high power density [209].

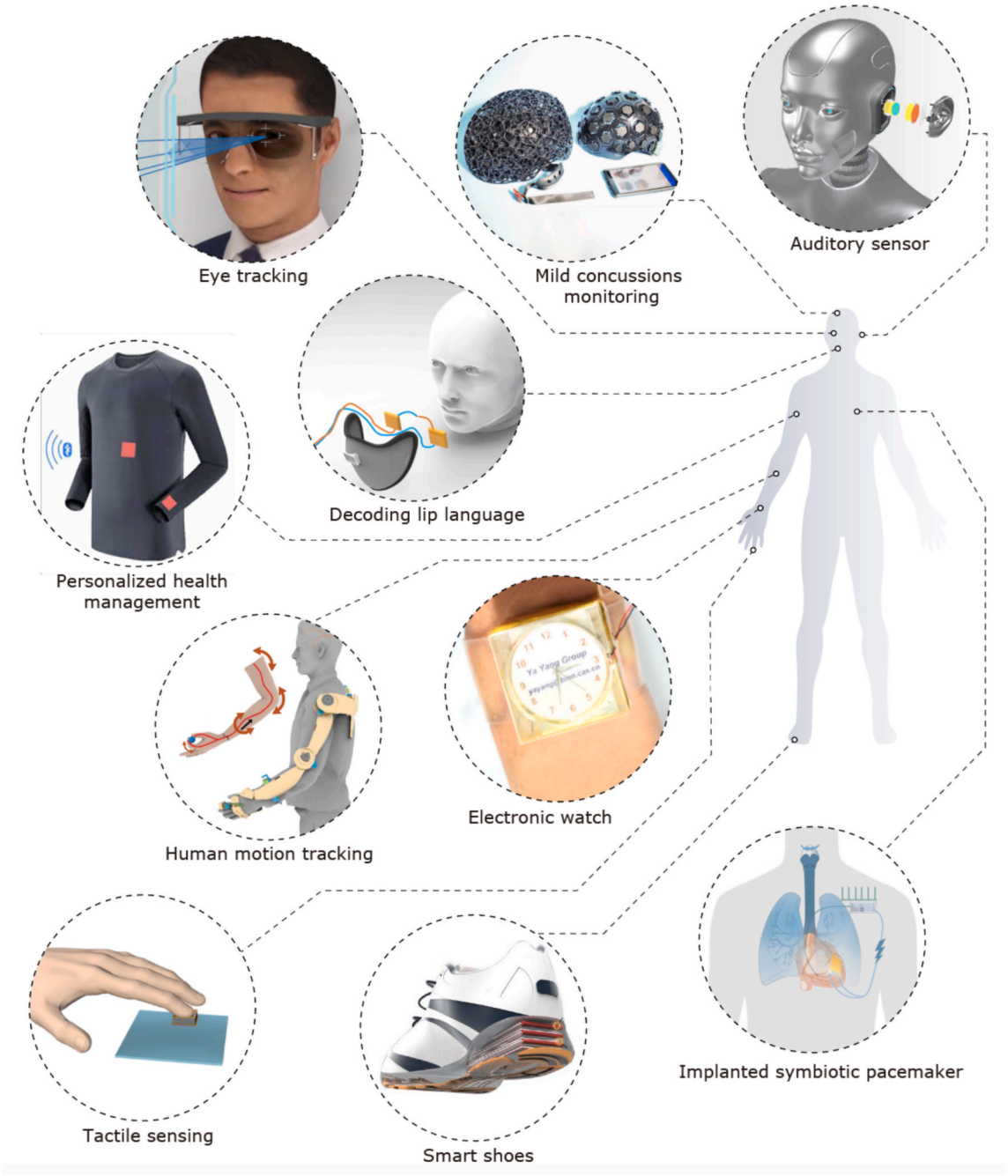

Fig. 8. Wearable electronic devices. Parts reprinted with permission [214]. Copyright 2023, Springer Nature. Parts reprinted with permission [213]. Copyright 2023, AAAS. Parts reprinted with permission [212]. Copyright 2018, AAAS. Parts reprinted with permission [216]. Copyright 2020, AAAS. Parts reprinted with permission [215]. Copyright 2022, Springer Nature. Parts reprinted with permission [217]. Copyright 2021, Springer Nature. Parts reprinted with permission [218]. Copyright 2015, ACS Publications. Parts reprinted with permission [219]. Copyright 2020, AAAS. Parts reprinted with permission [210]. Copyright 2015, Springer Nature. Parts reprinted with permission [221]. Copyright 2019, Springer Nature.

Other applications

Other applications such as implantable devices based on TENGs are also analyzed during these years. Ouyang and coworkers fabricated an implantable symbiotic pacemaker on basis of TENG, a power management module, and a pacemaker [221]. The output voltage of TENG can reach up to 65.2 V and the produced energy via each cardiac motion cycle is about 0.495 μJ. The pacemaker can be self-powed by scavenging the mechanical energy from heart beat, where the single heart beat can drive the pacemaker to work once. Ryu et al. reported a self-rechargeable cardiac pacemaker system by integrating a cardiac pacemaker with the enclosed five-stacked TENGs [222], where the produced electricity can be up to 4.9 μ W/cm^3. Moreover, a capacitive triboelectric electret was utilized to deliver a output voltage of 2.4 V and an output current of 156 μA by ultrasound energy transfer [44], showing the potential applications in implantable devices. Recently, Liu et al. demonstrated a battery-free, transcatheter pacemaker using TENG technology to harvest cardiac motion energy [220]. The capsule-shaped device (1.75 g, 1.52 cc) achieves in vivo open-circuit voltage of ~ 6.0 V and maintains pacing function for three weeks in swine models. This breakthrough addresses the energy limitations of implantable devices, offering a sustainable solution for arrhythmia treatment with minimal

surgical intervention.

Hui et al. proposed a triboelectric stethoscope with ultrahigh sensitivity (1215 mV Pa^{-1}), surpassing piezoelectric sensors by 60 times [223]. By designing a trumpet-shaped auscultatory cavity for acoustic energy converging, the device achieves a 36 dB signal-to-noise ratio in human tests and diagnoses five cardiac states with 97 % accuracy using machine learning. This work highlights TENG's potential in ultrasensitive biomedical sensing and non-invasive diagnostics. Imani et al. developed an implantable IBV-TENG with PHBV/PVA/Mg, generating 4 V/22 μA under ultrasound to inactivate 99 % E. coli and 100 % S. aureus in vitro, with controlled degradation in physiological environments [224].

Tan et al. introduced a dual-functional TENG capable of generating both high voltage and constant DC current for contactless charge injection into droplets [225]. This design enables manipulation of large-volume droplets (up to 3000 μL) with momentum up to 115.2 g mm s^{-1}, five times higher than traditional methods. The dual-functional TENG's unique structure integrates triboelectrification, electrostatic discharge, and induction, showcasing its versatility in non-slippery surface applications like chemical reactions and solid particle driving.

TENGs can deliver a high voltage without using transformer or power management circuit, which have potential applications in plasma excitation, air purification, and agricultural field. In a study conducted by Liu et al., it was demonstrated that the rotary freestanding TENG can directly drive the dielectric barrier discharge microplasma under different conditions [226]. The intensity and efficiency of the resulting discharge were found to be enhanced by adjusting the input frequency or gas thickness. The high voltages generated by TENGs can also produce ion pulses, which have practical applications in nanoelectrospray ionization and plasma discharge ionization for nano-coulomb molecular mass spectrometry [227]. By utilizing minimal samples, this technique enables mass spectrometry analysis with high sensitivity, achieving a detection limit of approximately 0.6 zeptomole for a 10 pg ml^{-1} cocaine sample. Guo et al. fabricated a TENG-based negative air ion generator [228], where carbon fiber electrodes ionize air molecules using the high output voltages from the TENG. This method achieved an electron–ion transformation efficiency of up to 97 %. Through employing this technology, the concentration of particulate matter in the air was significantly reduced from 999 to 0 ugm^{-3} in just 80 s, using a working frequency of 0.25 Hz. Furthermore, Li et al. demonstrated the use of TENGs driven by wind and rain energy to generate a self-generated high-voltage electric field. This field was found to improve the germination

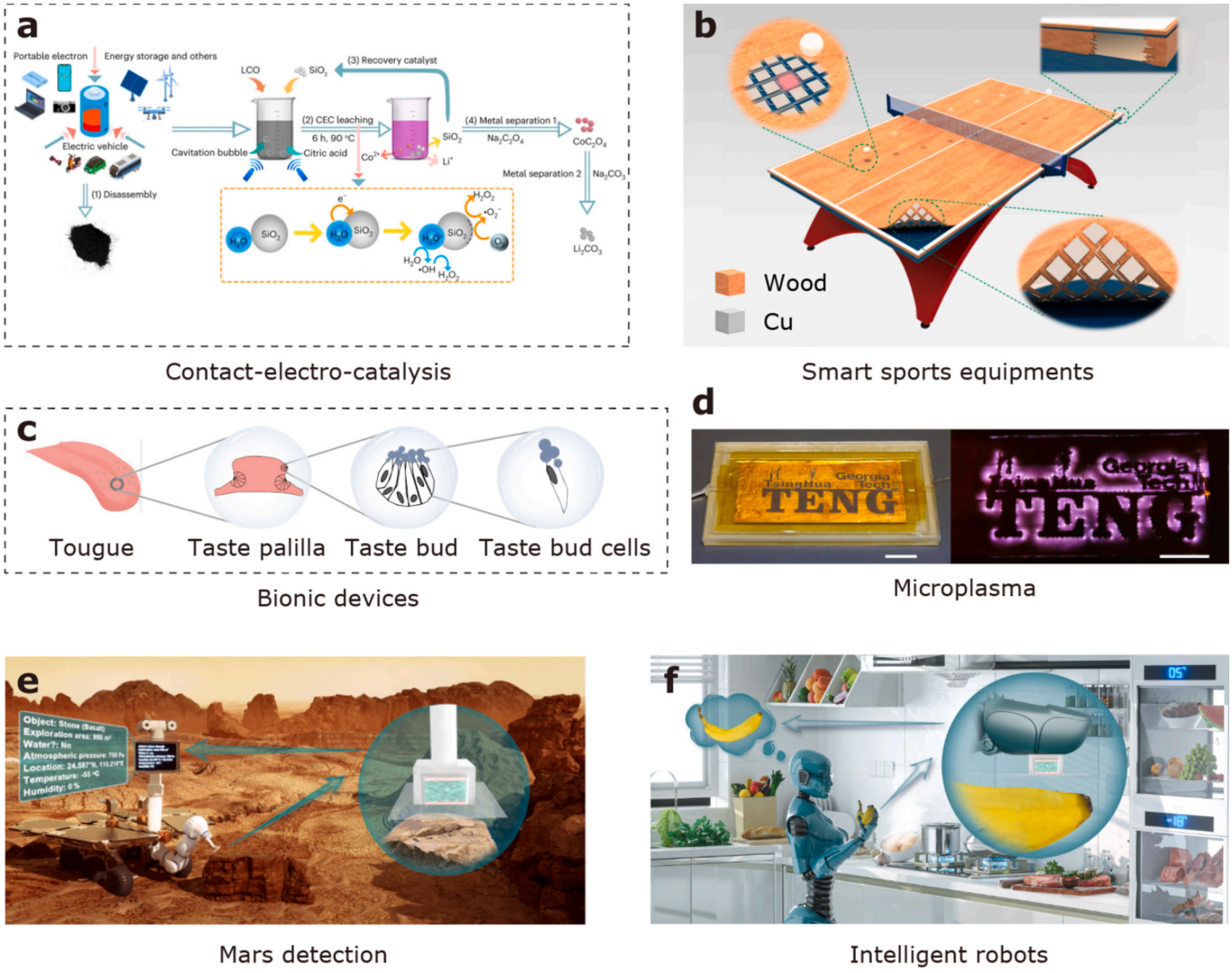

Fig. 9. Other applications. a, Contact-electro-catalysis. Reprinted with permission [229]. Copyright 2023, Springer Nature. b, Smart sports equipments. Reprinted with permission [230]. Copyright 2019, Springer Nature. c, Bionic devices. Reprinted with permission [231]. Copyright 2023, Springer Nature. d, Microplasma. Reprinted with permission [232]. Copyright 2018, Springer Nature. e, Mars detection. Reprinted with permission [233]. Copyright 2024, Springer. f, Intelligent robots. Reprinted with permission [233]. Copyright 2024, Springer.

speed of pea seeds by about 26.3 % and improve pea yield by about 17.9 % [196], providing a fresh direction of TENGs for agricultural production improvements. High voltage is used in power distribution to reduce ohmic losses when transporting electricity long distance. Besides, high voltage is used for generating electron beams for microscopy.

TENGs can have the other applications such as degradation of organic pollutants, smart sports equipments, and so on, as shown in Fig. 9. For instance, Li et al. introduced a mechano-catalytic approach utilizing ultrasonic waves to facilitate metal leaching, enabling recycling of Li-ion batteries [229]. Luo et al. presented a TENG-based self-powered falling point distribution statistical system and an edge ball judgment system [230]. These innovations have the potential to be applied in smart sport monitoring and big data analytics in intelligent sports fields. TENGs can be integrated into smart sports equipment to enable self-powered filling point distribution and accurate ball judgement [230]. They have also been employed as self-powered taste sensors for distinguishing between different liquids [231], and microplasma for patterned luminescence [232]. Moreover, the TENGs have been extensively used as tactile sensors. Wang and the coworkers fabricated a TENG based mulit-functional sensor that can achieve the material identification by using the TENG signals induced by different materials [219]. In the real-time operation of a soft robotic gripper process, TENGs were employed to identify diverse objects, achieving an impressive accuracy of 98.1 % [48]. By combining TENG and deep learning, the sensor can realize the accuracy of 90 % for the liquid recognition [231], where the recognition accuracy can be improved to 96 % by using an image sensor together. Shi and the coworkers reported TENG-based electro-tactile system by using TENG induced discharge current [51], which can reproduce the motion trace and potion on human skin. The applications of TENGs in Mars detection and intelligent robots also have been demonstrated [233], and more other new applications will be developed in future. We believe that TENGs will make more contributions to the development of human beings.

Recent breakthroughs in tribo-electro-catalysis have expanded TENGs' utility beyond energy harvesting [234]. For example, TENG-induced electric fields have been shown to enhance catalytic reactions for environmental remediation, such as degrading organic pollutants via triboelectrically activated reactive oxygen species [235]. This synergy between mechanical energy harvesting and electrochemical catalysis opens avenues for wastewater treatment systems. Additionally, TENG-driven probe techniques, such as liquid–solid triboelectric probes, enable monitoring of bubble status, providing insights into investigating tri-phase contact electrification dynamics [236].

In brief, TENGs bring benefits such as renewable energy harvesting, battery waste reduction, carbon emission mitigation, and sustainability. TENGs excel in capturing diverse mechanical motions such as human movement, wind, and water flow to produce electricity, thereby facilitating the adoption of renewable energy and diminishing dependence on conventional energy sources. Furthermore, TENG technology can autonomously power wearable gadgets and implantable medical devices, curtailing the necessity for disposable batteries and subsequently curbing battery waste. By diminishing the reliance on fossil fuels, TENG holds promise in curbing carbon emissions linked with traditional energy production, thereby contributing to endeavors aimed at combatting climate change. The integration of TENG harmonizes with the sustainable and eco-friendly objectives of clean technology. By harnessing ambient mechanical energy, TENG enables self-sufficient energy generation, thus propelling the progress of clean technology.

Outlook

In this review, we take on a systematic exploration of the latest advancements in the field of TENGs. Our analysis begins with a foundational overview of the core principles and theoretical underpinnings of TENGs, which includes the mechanisms of CE, the fundamental theory of TENG, as well as the diverse working modes that have been developed. Moreover, we delve into strategies aimed at augmenting the output performance of TENGs, recognizing the pivotal role this plays in facilitating their widespread application. While TENGs exhibit immense potential as a sustainable energy harvesting solution, there exists a pressing challenge in comprehensively enhancing their performance to cater to a broader spectrum of applications.

In spite of the extensively documented evidence showcasing electron transfer in diverse friction interfaces, such as solid–solid and solid–liquid interfaces, the precise characteristics of charge transfer species in different combinations of tribo-materials remain enigmatic and unexplored [123,124]. Moreover, within the context of triboelectric materials, the electron transfer occurring on their surfaces during the process of CE possesses the potential to initiate interfacial catalysis. This intriguing scientific question demands further investigation into how the charges generated through CE can influence the redox reactions occurring at the interface.

Although the existence of several strategies aimed at enhancing the performance of TENGs, there remains an urgent need to develop innovative methodologies and fabricate advanced materials to further elevate their performance [141,142]. For example, by optimizing the friction interface design, improving material structures, and exploring new nanomaterials, the performance of TENGs can be enhanced. Moreover, while emerging charge excitation methods offer promising avenues for significantly enhancing the performance of TENGs, they are still constrained due to air breakdown effect [136]. Therefore, the development of dielectric materials that possess high dielectric constants, ultrathin dimensions, and smooth surface structures has the potential to significantly increase the air breakdown threshold, thereby further boosting the output performance of TENGs [151].

Unlike prior studies focused on incremental material improvements, future research should prioritize: (1) ionic charge-dominated TENGs for high-humidity stability; (2) self-healing triboelectric materials to address mechanical wear; and (3) hybrid energy systems integrating TENGs with solar/wind technologies. These directions will solidify TENGs as a cornerstone of decentralized, low-carbon infrastructure, overcoming the scalability and environmental sensitivity challenges highlighted in existing reviews.

Currently, TENGs face significant commercialization challenges despite their clean energy potential. Environmental sensitivity causes drastic performance drops, where charge density falls over 50 % in high humidity [159], and mechanical wear degrades output power by 30 % [145]. Scalable manufacturing is hindered by costly precision techniques. High material costs and complex energy management systems limit competitiveness. Market adoption is slowed by user concerns over reliability and competition from mature technologies like solar cells. Regulatory hurdles include lacking performance standards and lengthy biocompatibility testing. Overcoming these requires interdisciplinary innovation in materials, fabrication, and policy.

Future research should prioritize emerging applications that leverage TENGs' unique capabilities. For example, high-temperature triboelectric materials could enable operation in extreme environments like industrial furnaces or space missions, building on the environmental control. In smart agriculture, TENGs could power self-sustaining soil sensors or use triboelectrically induced plasma for chemical-free pest control, expanding on the crop growth enhancement. In biomedical fields, ultra-sensitive TENG stethoscopes hold promise for non-invasive diagnostics, while triboelectric scaffolds may advance tissue engineering by modulating cell adhesion. For robotics, TENG-based tactile sensors could enhance soft grippers for delicate tasks. Hybrid energy systems, such as TENGs integrated with flexible solar cells, offer potential for continuous power supply in decentralized grids, addressing the intermittency challenges of low-frequency energy harvesting. Additionally, ionic charge-dominated designs may unlock underwater sensing or wearable devices for high-humidity environments, extending the marine and medical applications.

Over the past 10 years, TENG research has shifted from early-stage

concept validation to commercialization and industrial technology development. In 2024, TENG was selected into the "Top 10 Emerging Chemical Technologies" by the International Union of Pure and Applied Chemistry (IUPAC), marking a significant progress in its international recognition. Currently, key enterprises in the field include Inovenso, TEKTRONIX, INC., Bruker, Springer International Publishing AG, Newnagy, Shandong Linglong Tyre Co., InanoEnergy, Zolitron Technology, and NairTENG. Among them, the TENG tyre developed by Shandong Linglong Tyre in collaboration with Beijing University of Chemical Technology and the Chinese Academy of Sciences stands out as one of the most representative commercialized products. Leveraging the electrostatic properties of silica-based materials, this tyre converts mechanical energy generated from friction between the tire and the road into electrical energy while integrating a self-powered tire pressure monitoring function. At present, Shandong Linglong Tyre's triboelectric nanogenerator tire has undergone industry certification and entered the pilot phase, while InanoEnergy's wearable and medical products have achieved stable market supply. Other applications like self-powered mosquito repellers and smart textiles are still in the technical transformation or small-scale application stage. With continuous technological innovation and policy support, TENG products are expected to gradually transition from laboratory environments to a broader consumer market.

To bridge the gap between laboratory-scale advancements and real-world deployment, future efforts should prioritize interdisciplinary innovations that address TENGs' environmental sensitivity, mechanical durability, and scalability. For instance, the development of self-healing triboelectric materials, inspired by recent advances in dynamic covalent polymers, could mitigate performance degradation caused by mechanical wear. Simultaneously, designing ionic charge-dominated TENG architectures, leveraging insights from liquid-solid interfacial charge transfer mechanisms, may enhance stability in high-humidity environments. Hybrid energy systems integrating TENGs with solar or electromagnetic harvesters, could further optimize energy output under variable conditions. Scalable manufacturing techniques, such as roll-to-roll printing or biofabrication, must also be advanced to reduce costs while preserving nanoscale charge-trapping properties. Finally, establishing standardized protocols for evaluating TENG performance under real-world stressors will accelerate regulatory compliance and market adoption. These strategies, grounded in the fundamental principles and applications discussed herein, aim to transform TENGs into robust, versatile components of sustainable energy ecosystems.

CRediT authorship contribution statement

Ya Yang: Writing – original draft, Project administration. **Jie Wang:** Writing – original draft, Formal analysis. **Weiqi Qian:** Methodology. **Zhong Lin Wang:** Writing – review & editing, Supervision.

Declaration of competing interest

The authors declare that they have no known competing financial interests or personal relationships that could have appeared to influence the work reported in this paper.

Acknowledgments

This work was supported by the National Key R & D Project from the Minister of Science and Technology in China (No. 2021YFA1201601, No. 2021YFA1201604), the Beijing Natural Science Foundation (Grant No. JQ21007), and the National Natural Science Foundation of China (Grant No. 52072041).

Data availability

Data will be made available on request.

References

[1] L. Portilla, et al., Nat. Electron. 6 (2023) 10–17.
[2] H.W. Song, et al., Sci. Adv. 10 (2024) adl2882.
[3] J.E.T. Bistline, Joule 5 (2021) 2551–2563.
[4] S. Hur, et al., Nano Energy 114 (2023) 108596.
[5] F.R. Fan, Z.Q. Tian, Z.L. Wang, Nano Energy 1 (2012) 328–334.
[6] S. Krishnan, A. Giwa, J. Mater. Chem. A 13 (2025) 11134–11158.
[7] A. Baburaj, et al., Nano Energy 127 (2024) 109785.
[8] S. Liu, et al., Nano-Micro Lett. 17 (2025) 44.
[9] W.G. Kim, et al., ACS Nano 15 (2021) 328–334.
[10] T. Cheng, J. Shao, Z.L. Wang, Nat. Rev. Methods Primers 3 (2023) 39.
[11] M. Zhu, et al., ACS Nano 13 (2019) 1940–1952.
[12] K. Chen, et al., J. Mater. Chem. A 12 (2024) 3283–3293.
[13] Z.Q. Lu, et al., Nat. Commun. 15 (2024) 6513.
[14] P. Lu, et al., Nano-Micro Lett. 16 (2024) 206.
[15] L. Zhu, et al., Adv. Funct. Mater. 34 (2024) 2400363.
[16] X. Shi, et al., Small 20 (2023) 2307620.
[17] I. Ali, N. Karim, S. Afroj, EcoMat 6 (2024) e12471.
[18] Y.J. Kim, et al., Adv. Mater. 36 (2024) 2307194.
[19] X. Zhu, et al., Chem. Eng. J. 491 (2024) 152011.
[20] J. Wu, et al., Energy Environ. Sci. 18 (2025) 2381–2394.
[21] H. Chen, et al., Nano Energy 136 (2025) 110724.
[22] P. Sun, et al., Nano Energy 89 (2021) 106492.
[23] C. Zhu, et al., Adv. Sci. (2025) 2410289.
[24] Z. Che, et al., Small 19 (2023) 2207600.
[25] Y. Yun, et al., Nano Energy 80 (2021) 105525.
[26] L. Zhao, et al., InfoMat 6 (2024) e12520.
[27] Y. Li, et al., Adv. Sci. (2024) 2307382.
[28] J. He, et al., Small (2025) 2411074.
[29] L. Gao, et al., Nano Energy 127 (2024) 109697.
[30] J. Cao, et al., Small Methods 6 (2022) 2200588.
[31] W. Peng, et al., Adv. Energy Mater. 14 (2024) 2403289.
[32] X. Xia, et al., EcoMat 2 (2020) e12049.
[33] S. Xu, et al., J. Mater. Chem. A 13 (2025) 832–854.
[34] S. Dai, et al., InfoMat 5 (2023) e12391.
[35] Y. Zhang, et al., Nano Energy 135 (2025) 110674.
[36] S.Z. Liu, et al., Small 20 (2024) 2405520.
[37] Z. Sun, et al., Adv. Sci. 8 (2021) 2100230.
[38] Y. Yang, et al., ACS Nano 7 (2013) 9213–9222.
[39] J. Chen, et al., Nat. Energy 1 (2016) 16138.
[40] Z. Xu, et al., Nat. Commun. 14 (2023) 2792.
[41] Y. Yang, et al., ACS Nano 7 (2013) 9461–9468.
[42] F.R. Fan, et al., ACS Nano 12 (2012) 3109–3114.
[43] W. Seung, et al., ACS Nano 12 (2012) 3109–3114.
[44] R. Hinchet, et al., Science 365 (2019) 491–494.
[45] C. Zhang, et al., Joule 5 (2021) 1–11.
[46] C. Li, et al., Nat. Commun. 12 (2021) 2950.
[47] W. Li, et al., Nat. Commun. 8 (2017) 15310.
[48] T. Jin, et al., Nat. Commun. 11 (2020) 5381.
[49] Y. Zou, et al., Nat. Commun. 10 (2019) 2695.
[50] R. Liu, et al., Nat. Rev. Mater. 7 (2022) 870–886.
[51] Y. Shi, et al., Sci. Adv. 7 (2021) eabe2943.
[52] C. Wang, et al., Adv. Mater. 35 (2023) 2209895.
[53] F. Jiang, et al., Adv. Mater. 36 (2024) 2308197.
[54] C. Wu, et al., Adv. Energy Mater. 9 (2019) 1802906.
[55] Z.L. Wang, J. Chen, L. Lin, Energy Environ. Sci. 8 (2015) 2250–2282.
[56] J. Chen, Z.L. Wang, Joule 1 (2017) 480–521.
[57] Q. Zheng, et al., Nat. Rev. Cardiol. 3 (2023) 39.
[58] Y. Su, et al., Adv. Mater. 33 (2021) 2101262.
[59] Y. Yang, et al., Adv. Energy Mater. 3 (2013) 1563–1568.
[60] Y.J. Kim, et al., Nat. Water 2 (2024) 360–369.
[61] Z.L. Wang, et al., Triboelectric Nanogenerators, Springer, 2016.
[62] Z.L. Wang, Adv. Energy Mater. 10 (2020) 2000137.
[63] D. Wang, et al., ACS Nano 15 (2021) 2911–2919.
[64] X. Meng, et al., Nano Energy 127 (2024) 109716.
[65] W. Liu, Z. Wang, C. Hu, Mater. Today 45 (2021) 93–119.
[66] C. Shan, et al., Energy Environ. Sci. 14 (2021) 5395–5405.
[67] C. Rodrigues, et al., Energy Environ. Sci. 13 (2020) 2657–2683.
[68] Z. Wang, et al., Joule 5 (2021) 441–455.
[69] H. Xiang, et al., Sci. Adv. 10 (2024) ads2291.
[70] X. Cao, et al., Nano-Micro Lett. 15 (2023) 14.
[71] D. Choi, et al., Nano Energy 36 (2017) 250–259.
[72] L. Jin, et al., Nano Lett. 20 (2020) 6404–6411.
[73] Q. Zhang, et al., Adv. Mater. 29 (2017) 1606703.
[74] Y. Liu, et al., Adv. Funct. Mater. 30 (2020) 2004714.
[75] Y.S. Zhou, et al., Nano Lett. 13 (2013) 2771–2776.
[76] W. He, et al., Adv. Energy Mater. 12 (2022) 2201454.
[77] H. Wu, et al., Adv. Energy Mater. 13 (2023) 2300051.
[78] J. Chen, et al., Mater. Interfaces 8 (2016) 736–744.
[79] G. Zhao, et al., Nano Energy 59 (2019) 302–310.
[80] M. Wang, et al., J. Mater. Chem. A 5 (2017) 12252–12257.
[81] P. Zhao, et al., Mater. Interfaces 10 (2018) 5880–5891.
[82] Y. Feng, et al., Nano Energy 38 (2017) 467–476.
[83] J. Son, et al., Adv. Sci. 10 (2023) 2301609.
[84] M. Zhang, et al., Nano Energy 30 (2016) 155–161.

[85] R. Ouyang, et al., Nano Energy 102 (2022) 107749.
[86] Y. Yu, et al., Mater. Today 64 (2023) 61–71.
[87] Z. Zhao, et al., Nat. Commun. 12 (2021) 4686.
[88] C. Xu, et al., Adv. Mater. 30 (2018) 1706790.
[89] H. A. Radi, J. O. Rasmussen, Electric Force. In: Principles of Physics (Springer, 2013).
[90] J. Wu, et al., Nano Energy 63 (2019) 103864.
[91] A. Berbille, et al., Adv. Mater. 35 (2023) 2304387.
[92] X. Xia, et al., Nano Energy 78 (2020) 105343.
[93] J. Wu, et al., Nano Energy 48 (2018) 607–616.
[94] G. Grosjean, S. Waitukaitis, Phys. Rev. Lett. 130 (2023) 098202.
[95] A. Šutka, et al., Energy Environ. Sci. 12 (2019) 2417–2421.
[96] S. Lin, et al., Nat. Commun. 11 (2020) 399.
[97] Z.H. Lin, et al., Angew. Chem. Int. Ed. 52 (2013) 12545–12549.
[98] Z.L. Wang, A.C. Wang, Mater. Today 30 (2019) 34–51.
[99] X. Zhao, et al., Nano Energy 87 (2021) 106191.
[100] M. Willatzen, Z.L. Wang, Nano Energy 52 (2018) 517–523.
[101] M. Willatzen, Z.L. Wang, Nano Energy 61 (2019) 311–317.
[102] C. Xu, et al., Adv. Funct. Mater. 29 (2019) 1903142.
[103] A.C. Wang, et al., Adv. Funct. Mater. 30 (2020) 1909384.
[104] S. Lin, et al., Adv. Funct. Mater. 30 (2020) 1909724.
[105] J.S.C. Koay, et al., J. Mater. Chem. A 8 (2020) 25857–25866.
[106] C. Xu, et al., Adv. Mater. 30 (2018) 1802968.
[107] Z.L. Wang, Rep. Prg. Phys. 84 (2021) 096502.
[108] G. Xu, et al., Mater. Interfaces 14 (2022) 5355–5362.
[109] S. Lin, et al., Nat. Commun. 13 (2022) 5230.
[110] J. Hu, M. Iwamoto, X. Chen, Nano-Micro Lett. 16 (2024) 7.
[111] D. Li, et al., Sci. Adv. 7 (2021) eabj0349.
[112] W. Zhang, et al., Front. Mater. 9 (2022) 909746.
[113] Y. Chen, et al., ACS Nano 13 (2019) 8936–8945.
[114] Y. Wei, et al., Mater. Today 74 (2024) 2–11.
[115] Y. Zhao, et al., Nano Energy 112 (2023) 108464.
[116] J. Dong, et al., Nano Energy 95 (2022) 10691.
[117] L. Zhang, et al., Nano Energy 78 (2020) 105370.
[118] S. Lin, X. Chen, Z.L. Wang, Chem. Rev. 122 (2022) 5209–5232.
[119] I.Y. Suh, et al., Electron. Mater. 6 (2024) 4826–4842.
[120] J. Nie, et al., Adv. Mater. 32 (2019) 1905696.
[121] S. Lin, M. Zheng, Z.L. Wang, J. Phys. Chem. C 125 (2021) 14098–14104.
[122] Z.L. Wang, Mater. Today 52 (2022) 348–363.
[123] H. Zhao, et al., Nat. Commun. 13 (2022) 3325.
[124] Z.L. Wang, Mater. Today 20 (2017) 74–82.
[125] Z.L. Wang, Nano Energy 68 (2020) 104272.
[126] Z.L. Wang, Intern. J. Mod. Phys. B 37 (2022) 2350159.
[127] Z.L. Wang, J. Shao, Electromagn. Sci. 1 (2023) 0020171.
[128] L.A. Zhang, et al., Energy Environ. Sci. 16 (2023) 3781–3791.
[129] S. Zhang, et al., Nano Energy 130 (2024) 110093.
[130] Y. Zi, et al., Nat. Commun. 6 (2015) 8376.
[131] J. Shao, et al., Nano Energy 51 (2018) 688–697.
[132] K. Dai, et al., Nano Res. 10 (2017) 157–171.
[133] S. Cui, et al., Nano Energy 112 (2023) 108509.
[134] Y. Lyu, Y. Wang, Nano Energy 103 (2022) 107811.
[135] R. Dharmasena, S.R.P. Silva, Nano Energy 62 (2019) 530–549.
[136] R. Lei, et al., Adv. Energy Mater. 12 (2022) 2201708.
[137] X. Liang, et al., Adv. Energy Mater. 10 (2020) 2002123.
[138] V. Nguyen, R. Yang, Nano Energy 2 (2013) 604–608.
[139] W. Qian, et al., ACS Energy Lett. 9 (2024) 1907–1914.
[140] H. Zhang, J. Mater. Chem. A 11 (2023) 24454–24481.
[141] H. Zou, et al., Nat. Commun. 10 (2019) 1427.
[142] D. Liu, et al., Nat. Commun. 13 (2022) 6019.
[143] D. Han, et al., Adv. Funct. Mater. 35 (2025) 2501362.
[144] G. Pace, et al., Adv. Mater. 35 (2023) 2211037.
[145] Y. Yu, et al., Joule 8 (2024) 1855–1868.
[146] B. Liu, et al., Nano Energy 130 (2024) 110094.
[147] L. Xu, et al., Nano Energy 49 (2018) 625–633.
[148] L. Cheng, et al., Nat. Commun. 9 (2018) 3773.
[149] W. Liu, et al., Nat. Commun. 10 (2019) 1426.
[150] Y. Liu, et al., Nat. Commun. 11 (2020) 1599.
[151] H. Wu, et al., Adv. Mater. 34 (2022) 2109918.
[152] H. Wu, et al., Energy Environ. Sci. 16 (2023) 2274–2283.
[153] J. Wang, et al., Energy Environ. Sci. 17 (2024) 7382–7393.
[154] T. Kuang, et al., Adv. Mater. 37 (2025) 2415616.
[155] X. Yang, et al., Nano Energy 60 (2019) 404–412.
[156] Y. Pang, et al., Nano Energy 114 (2023) 108659.
[157] J. Wang, et al., Nat. Commun. 8 (2017) 88.
[158] J. Fu, et al., Adv. Sci. 7 (2020) 2001757.
[159] K. Wang, et al., Nano Energy 93 (2022) 106880.
[160] L. Liu, et al., J. Mater. Chem. A 9 (2021) 21357–21365.
[161] S. Lin, et al., Adv. Mater. 31 (2019) 1808197.
[162] B. Cheng, et al., Nat. Commun. 12 (2021) 4782.
[163] X. Xia, et al., Nature Commun. 14 (2023) 1023.
[164] Z.L. Wang, Faraday Discuss. 176 (2014) 447–458.
[165] J. Luo, Z.L. Wang, EcoMat 2 (2020) e12059.
[166] V. Zacharia, et al., Nano Energy 127 (2024) 109702.
[167] G. Li, et al., Energy Environ. Sci. 17 (2024) 2651–2661.
[168] Y. Li, et al., Nano Energy 125 (2024) 109515.
[169] L. Chen, et al., Chem. Eng. J. 488 (2024) 150891.
[170] Y. Wang, et al., Nat. Commun. 15 (2024) 6834.
[171] D. Liu, et al., Sci. Adv. 5 (2019) eaav6437.
[172] S. Zhang, et al., Nano Energy 139 (2025) 110947.
[173] Z. Zhang, et al., Adv. Energy Mater. 10 (2020) 1903713.
[174] X. Yin, et al., Adv. Mater. 37 (2025) 2417254.
[175] D. Bhattacharya, et al., Adv. Funct. Mater. 34 (2024) 2403705.
[176] Y. Yang, et al., ACS Nano 7 (2013) 9461–9468.
[177] L. Zhang, et al., Nano Energy 95 (2022) 107029.
[178] J. Bae, et al., Nat. Commun. 5 (2014) 4929.
[179] Z. Ren, et al., Nano Energy 100 (2022) 107522.
[180] X. Tang, et al., Nano Energy 99 (2022) 107412.
[181] D. Yang, et al., Nano Energy 90 (2021) 106641.
[182] L. He, et al., ACS Nano 16 (2022) 6244–6254.
[183] J. Wang, et al., ACS Nano 12 (2018) 3954–3963.
[184] S. Lu, et al., Nano Energy 75 (2020) 104813.
[185] X. Li, et al., Appl. Energy 306 (2022) 117977.
[186] X. Li, et al., Nano Energy 128 (2024) 109965.
[187] Q. Zheng, et al., Nano Energy 97 (2022) 107183.
[188] I. Mehamud, et al., Nano Energy 98 (2022) 107292.
[189] Y. Wang, et al., Nano Energy 78 (2020) 105279.
[190] H.R. Zhu, et al., Nano Energy 14 (2015) 193–200.
[191] Z. Zhu, et al., Nano Energy 93 (2022) 106776.
[192] Z. Ren, et al., Adv. Energy Mater. 10 (2020) 2001770.
[193] S. Wang, et al., ACS Nano 9 (2015) 9554–9563.
[194] B. Chen, Y. Yang, Z.L. Wang, Adv. Energy Mater. 8 (2017) 1702649.
[195] S. Wang, et al., ACS Nano 10 (2016) 5696–5700.
[196] X. Li, et al., Nat. Food 3 (2022) 133–142.
[197] Z.L. Wang, Nature 542 (2017) 159–160.
[198] Y. Feng, et al., Adv. Energy Mater. 12 (2021) 2103143.
[199] H. Wang, et al., Nano Energy 84 (2021) 105920.
[200] H. Wang, et al., Nat. Commun. 11 (2020) 4203.
[201] S.L. Zhang, et al., Nano Energy 84 (2021) 421–429.
[202] M. Xu, et al., ACS Nano 13 (2019) 1932–1939.
[203] T.X. Xiao, et al., Adv. Funct. Mater. 28 (2018) 1802634.
[204] C. Zhang, et al., Adv. Energy Mater. 11 (2021) 2003616.
[205] W. Yuan, et al., One Earth 5 (2021) 1055–1063.
[206] X. Peng, et al., Sci. Adv. 6 (2020) eaba9624.
[207] K. Dong, et al., Nat. Commun. 11 (2020) 2868.
[208] Q. Jing, et al., Nat. Commun. 6 (2015) 8031.
[209] J. Wang, et al., Nat. Commun. 7 (2016) 12744.
[210] S. Niu, et al., Nat. Commun. 6 (2015) 8975.
[211] J. Yu, et al., Nat. Commun. 12 (2021) 1581.
[212] H. Guo, et al., Sci. Robotics 3 (2018) eaat2516.
[213] L. Zu, et al., Sci. Adv. 9 (2023) eadg5152.
[214] Y. Shi, et al., Nat. Commun. 14 (2023) 3315.
[215] Y. Lu, et al., Nat. Commun. 13 (2022) 1401.
[216] W. Fan, et al., Sci. Adv. 6 (2020) eaay2840.
[217] M. Zhu, et al., Nat. Commun. 12 (2021) 2692.
[218] T. Quan, et al., ACS Nano 9 (2015) 12301–12310.
[219] Y. Wang, et al., Sci. Adv. 6 (2020) eabb9083.
[220] Z. Liu, et al., Nat. Commun. 15 (2024) 507.
[221] H. Ouyang, et al., Nat. Commun. 10 (2019) 1821.
[222] H. Ryu, et al., Nat. Commun. 12 (2021) 4374.
[223] X. Hui, et al., Adv. Mater. 36 (2024) 2401508.
[224] I.M. Imani, et al., Adv. Sci. 10 (2023) 2204801.
[225] L. Tan, et al., Adv. Mater. 36 (2024) 2313878.
[226] F. Liu, et al., Nano Energy 56 (2019) 482–493.
[227] A. Li, et al., Nat. Nanotechnol. 12 (2017) 481–487.
[228] H. Guo, et al., Nat. Sustain. 4 (2021) 147–153.
[229] H. Li, et al., Nat. Energy 8 (2023) 1137–1144.
[230] J. Luo, et al., Nat. Commun. 10 (2019) 5147.
[231] X. Wei, et al., Nat. Food 4 (2023) 721–732.
[232] J. Cheng, et al., Nat. Commun. 9 (2018) 3733.
[233] H. Zhao, et al., Nano-Micro Lett. 16 (2024) 11.
[234] X. Li, W. Tong, J. Mater. Chem. A 12 (2024) 19783–19805.
[235] F. Dong, et al., Small (2025) 2500369.
[236] B. Luo, et al., Adv. Funct. Mater. 34 (2024) 2315725.